To the Graduate Council:

I am submitting herewith a thesis written by David Ernest Jackson entitled "Petrogenesis of a Shallow-Level Kimberlite From Taughannock Creek, New York." I have examined the final copy of this thesis for form and content and recommend that it be accepted in partial fulfillment of the requirements for the degree of Master of Science, with a major in Geology.

Lawrence A. Taylor
Lawrence A. Taylor, Major Professor

We have read this thesis
and recommend its acceptance:

Accepted for the Council:

L Evans Bell
Vice Chancellor
Graduate Studies and Research

PETROGENESIS OF A SHALLOW-LEVEL KIMBERLITE FROM TAUGHANNOCK CREEK, NEW YORK

A Thesis

Presented for the

Master of Science

Degree

The University of Tennessee, Knoxville

David Ernest Jackson

December 1982

ACKNOWLEDGEMENTS

Dr. Lawrence A. Taylor, my thesis advisor, provided generous support, instructive guidance, and an abiding confidence in my abilities throughout my graduate tenure at The University of Tennessee. I am especially indebted to Dr. Robert H. Hunter of Edinburgh, Scotland whose time-saving advice facilitated my research, and whose critical comments greatly enhanced the content of this work. Members of my thesis committee, Dr. Otto C. Kopp and Dr. Harry Y. McSween also provided helpful critical reviews of my manuscript; they very kindly set aside time for a summer defense date. Also appreciated is the expertise of Ronnie McKamey who kept a temperamental electron microprobe in good working order.

Thanks are in order for several others: friends and colleagues at UT whose association I have enjoyed throughout my stay in graduate school. My parents, Mr. and Mrs. Charles P. Jackson, Jr. of Nashville, Tennessee have shown me a lifetime of diligent love and support. Mr. E.T. Horn of Newport Beach, California provided me with generous encouragement and sound counsel. Most importantly, thanks to my wife and closest companion, Brenda, for indulging a year of my late nights and kimberlite-oriented weekends.

Financial assistance for this project was provided through NASA Grant NGL 43-001-140. Public presentations of this work at national scientific meetings were supported in part by the Discretionary Fund, Department of Geological Sciences, The University of Tennessee.

ABSTRACT

The petrogenesis of kimberlite from Taughannock Creek, near Ithaca, New York, can be separated into three distinct stages. Stage 1 comprises the evolution of kimberlitic melt within the upper mantle. Fractionation of olivine, Cr-pyrope, Cr-diopside, enstatite, and Cr-Al-spinel occurred over the temperature interval 950-1350° C in the depth range from 95 km to within the spinel stability field (< 70 km). Spinel peridotite xenoliths were incorporated during this stage. Picroilmenite is absent as a megacryst phase. The geothermobarometric estimates indicate that fractionation within this kimberlite occurred above the low velocity zone, significantly shallower than the typical kimberlite source region. This shallow origin may account for the paucity of picroilmenite, a ubiquitous phase in deeper kimberlites. During its passage through the shallow upper mantle or lower crust (Stage 2) the kimberlite disrupted an eclogitic body incorporating xenocrysts of Cr-poor diopside, almandine, and mineralogically similar eclogite xenoliths. Back-reaction with the more primitive kimberlitic melt produced reverse zoned rims on some xenocrysts. The typical kimberlitic paragenetic sequence Cr-spinel - Ti-magnetite - perovskite is present in the groundmass oxides, reflecting Cr-depletion and Ti-, Fe^{3+}-, and Ca-enrichment during the kimberlite's later stages of development. The passive, near surface emplacement (Stage 3) of the kimberlite as narrow dikes along North-South joint planes is probably a function of rift-related tectonic activity associated with the opening of the proto-North Atlantic Ocean.

TABLE OF CONTENTS

LIST OF TABLES

LIST OF FIGURES

CHAPTER I

INTRODUCTION

Kimberlites are rare ultramafic rocks that contain significant quantities of mantle-derived minerals. These minerals are important because they provide data pertinent to the understanding of the physiochemical properties of the upper mantle (e.g., Boyd and Nixon, 1975; MacGregor, 1979; Eggler et al., 1979; Ehrenburg and Griffin, 1979). Additionally, petrographic and chemical analyses of the minerals and rock assemblages contained in a kimberlite permit the reconstruction of its petrologic evolution. In order to understand this petrogenesis, it is necessary to evaluate all of a kimberlite's features, including evidence for fractionation and assimilation, the nature and origin of various crustal xenoliths, and even the implications of the tectonic regime permitting its birth.

Although a strict definition of the characteristics of kimberlitic rocks has not been universally agreed upon, there is a consensus among workers regarding the identity of the more salient features of these rocks (e.g., Skinner and Clement, 1979; Dawson, 1980; Pasteris, 1981). Kimberlites have been described as porphyritic rocks comprising a modal predominance of olivine, plus several of the following phases: calcite, serpentine, phlogopite, perovskite, picroilmenite, Mg-garnet, Cr-diopside, and monticellite. Additionally, it is recognized that many of these phases, occurring as megacrysts and in ultramafic xenoliths, yield estimates of pressure and temperature of equilibration which correspond to depths ranging from 80 to 200 km -- an origin within

the low velocity zone of the mantle. The chemistry and textures of oxide minerals in kimberlite characteristically reflect late-stage increases in Ca and Ti activities (e.g., Haggerty et al., 1979; Pasteris, 1981; Agee et al., 1982). Kimberlites are most commonly emplaced as diatremes, or as dikes and sills (Dawson, 1967).

Kimberlites are sparsely distributed throughout the eastern United States, generally following a trend that parallels the Appalachian Plateau from Tennessee to New York (Meyer, 1976). These small intrusives range in age from Permian to Jurassic (Zartmann et al., 1967; Pimentel et al., 1975). Recent work in this region includes research conducted on kimberlite occurrences in Kentucky (e.g., Garrison and Taylor, 1980; Agee et al., 1982), Pennsylvania (Kissling, et al., 1981; Hunter and Taylor, 1982a; 1982b) and New York (Foster, 1970; Snedden and Kay, 1981a; 1981b; Jackson et al., 1982a; 1982b).

Over eighty occurrences of hypabyssal-facies kimberlite are exposed in the Finger Lake region of New York State (Foster, 1970). The Central New York kimberlites were first noted by Vanauxem (1837). Subsequent research consisted mainly of general physiographic and petrographic descriptions, which classified the intrusives variously as mica peridotite, alnoite, and kimberlite (Kemp, 1891; Matson, 1905; Barnett, 1905; Martens, 1924; Maynard and Polger, 1946). Foster (1970) focused research on the general mineralogy and mode of emplacement of dikes from several New York localities. A K-Ar date of 145± 7 million years was determined for one Central New York kimberlite by Zartmann et al. (1967). Basu and Rubury (1980) have discussed the tectonic significance of the kimberlite occurrences of this region. Most

recently, Snedden and Kay (1981) conducted geochemical studies on three New York kimberlites, one of which was the Taughannock Creek occurrence.

The ten dikes occurring in Taughannock Creek near the west shore of Lake Cayuga (Figure 1) are the subject of the present study. The Taughannock Creek dikes are distributed over a 1 km interval (Figure 2). They are oriented generally parallel to the regional joint system that trends North-South (Foster, 1970). This orientation is typical of kimberlite dikes in the Central New York area. The Taughannock Creek dikes, ranging in width from 3 to 20 cm, intrude flat-lying, Devonian shales and exhibit three modes of occurrence: (1) massive intrusions that are strictly confined to joint planes; (2) intrusions that essentially follow jointing, but lack massive structure; these dikes contain shale xenoliths that have spalled off the surrounding country rock; (3) least commonly, highly brecciated dikes that diverge from joint patterns and contain numerous shale clasts; these intrusions may be anastomozed and frequently display limited lateral injection into the country rock. The kimberlite, brownish-green in color, is tough, well-indurated rock, unlike the unconsolidated soils typical of many kimberlites in which weathering is more advanced (e.g., the Norris, Tennessee intrusion). Despite extensive serpentinization, several dikes contain unaltered, primary phases. The petrography and chemistry of these minerals record changes in physiochemical conditions within the magmatic environment. The present study presents detailed petrographic and chemical analyses of these mineral constituents and synthesizes these data into a model for the petrogenetic history of the Taughannock Creek kimberlite.

Figure 1. Location map of Taughannock Creek, New York.

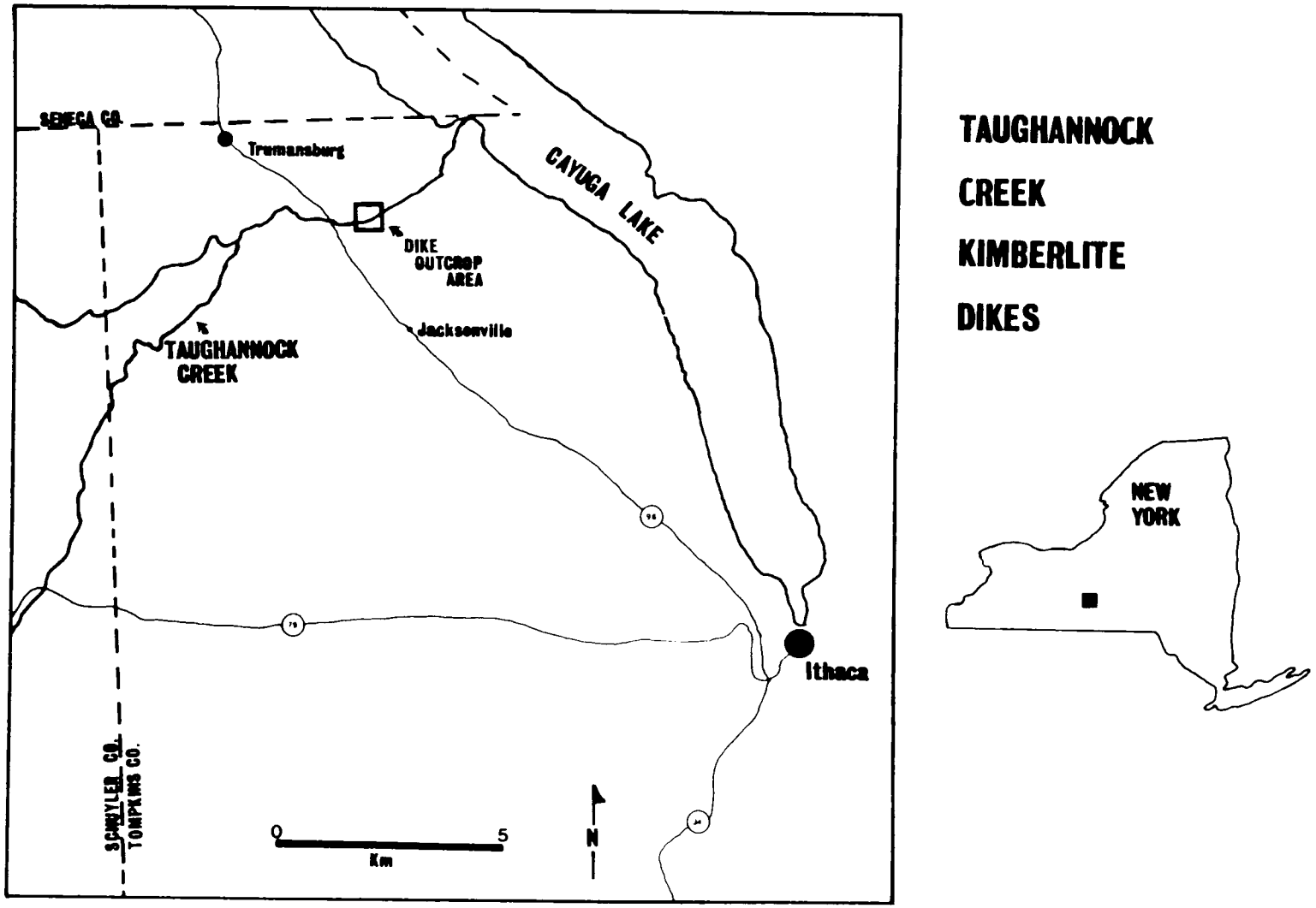
SENECA CO.
Trumansburg
CAYUGA LAKE
DIKE
OUTCROP
AREA
Jacksonville
TAUGHANNOCK
CREEK
Ithaca
SCHUYLER CO.
TOMPKINS CO.
0
5
Km
N
TAUGHANNOCK
CREEK
KIMBERLITE
DIKES
NEW
YORK

Figure 1.

Figure 2. Detail map of Taughannock Creek showing areal distribution of kimberlite dikes.

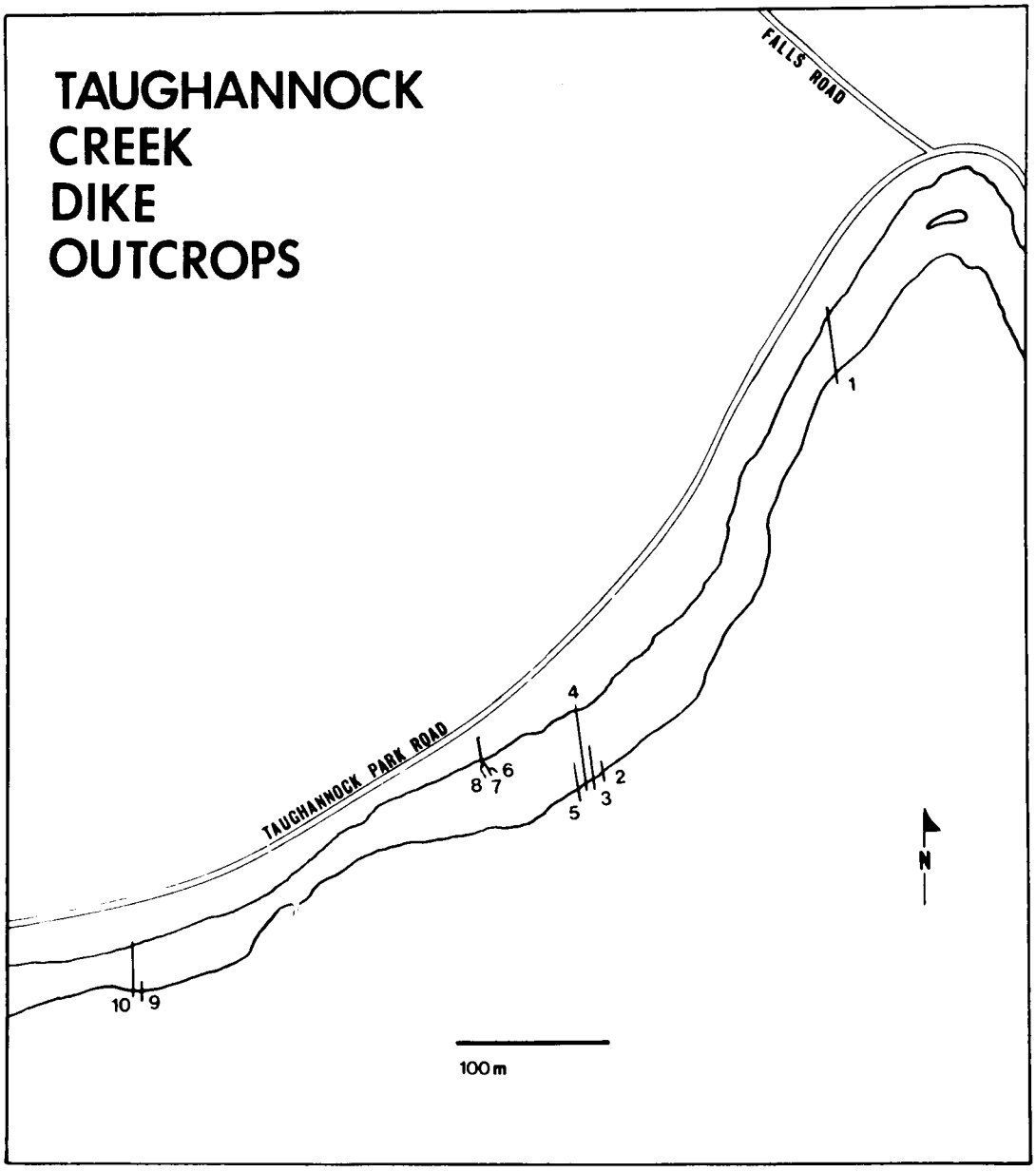
TAUGHANNOCK
CREEK
DIKE
OUTCROPS
FALLS ROAD
TAUGHANNOCK PARK ROAD
1
2
3
4
5
6
7
8
9
10
N
100 m

Figure 2.

Methods

Samples were collected from the eight widest dikes in Taughannock Creek (nos. 1, 3, 4, 5, 6, 7, 8, 10; Figure 2). These samples were serially slabbed and examined under a binocular microscope, after which 110 polished thin sections and 5 probe mounts were produced. Petrographic analyses employed both transmitted and reflected light techniques.

Chemical analyses of minerals were performed on an automated MAC 400S electron microprobe utilizing the correction procedures of Bence and Albee (1968) and the data of Albee and Ray (1970). Analyses were conducted using both natural and synthetic standards. An excitation potential of 15 KeV was used throughout the analyses. Depending on the nature of the sample material, the beam current was set at 0.04 to 0.05 microamps and the beam diameter was focused to 1 to 3 microns. Whenever grain size permitted, 3 to 10 analyses were conducted on each grain and an average and 1σ standard deviation were computed. Traverses from core to rim were made on clinopyroxenes, garnets, spinels, and phlogopites. Fe^{3+} content in oxides was calculated on the basis of stoichiometry.

CHAPTER II

PETROGRAPHY

The Taughannock Creek kimberlite contains megacrysts (relative abundances: serpentinized olivine >>phlogopite > garnet > clinopyroxene > spinel > enstatite) and mantle and crustal xenoliths set in a groundmass consisting of serpentinized olivine, phlogopite, euhedral spinels, carbonate, and various hydrous silicates (e.g. chlorite). The term "megacryst", texturally synonymous with "phenocryst" and "xenocryst", avoids the genetic connotations implicit in these latter terms. In this study, all crystals larger than groundmass size (> 0.02 cm) are referred to as megacrysts.

Typically, these rocks exhibit flow alignment of groundmass phlogopites and a heterogeneous distribution of porphyritic phases; these textures are typical of hypabyssal-facies kimberlites (e.g., Dawson and Hawthorne, 1970). Other textures in these dikes which are formed during kimberlite dike emplacement include well-developed rounding of megacrysts and xenoliths (indicative of fluidization and rapid, forceful ascension) and kinking and shearing of megacryst phlogopite laths (compression textures).

Although Foster (1970) reported the occurrence of unaltered olivine in a portion of Dike 10 in Taughannock Creek, the present study has revealed no preserved olivine in any of the dikes sampled. Alteration of olivine to serpentine, phlogopite, and calcite is pervasive. The serpentine pseudomorphs indicate that olivine was present as rounded to euhedral megacrysts (0.02 - 1.2 cm in diameter)

which contain secondary magnetite associated with serpentinization. In addition, serpentinized olivine is present in spinel peridotite xenoliths.

Garnet occurs as rounded megacrysts (0.05 - 1.2 cm in size; Figure 3a) and as intergrowths in eclogite nodules and clinopyroxene megacrysts. In hand sample, garnet megacrysts can be distinguished on the basis of color: pyrope appears reddish-purple; almandine is pink-orange. Both types are surrounded by kelyphitic reaction rims comprising intergrowths of hydrous silicates and spinels (Figure 3a). Along fractures within garnets, phlogopite with inclusions of Cr-spinel is present. Some garnet megacrysts host rounded inclusions of enstatite and diopside, 50 - 100 μm in size (Figure 3b). Additionally, garnet occurs as both elongate and granular inclusions (200 - 300 μm wide) in clinopyroxene megacrysts. Some of these inclusions appear to have been partially replaced by plagioclase. These textures are similar to those reported in eclogite from the Roberts Victor kimberlite in South Africa (Harte and Gurney, 1975). A description of nodular intergrowths of garnet and clinopyroxene is included in the discussion on xenoliths (see below).

Both clino- and orthopyroxene are present. Clinopyroxene occurs as rounded megacrysts (0.04 - 0.8 cm in size) (Figure 4), as constituents of eclogite and spinel peridotite xenoliths, and as inclusions in garnet megacrysts. Some of the clinopyroxene megacrysts exhibit fretted margins surrounded by intergrowths of phlogopite. A few megacysts possess thin rims, up to 100 μm wide, optically discontinuous with the core. Inclusions of rutile rodlets (50 μm in size)

Figure 3. Transmitted-light photomicrographs of garnet megacrysts. Scale bar = 500 μm.

a. Megacryst mantled by kelyphitic rim.

b. Garnet megacryst hosting inclusions of clinopyroxene (cpx) and orthopyroxene (opx).

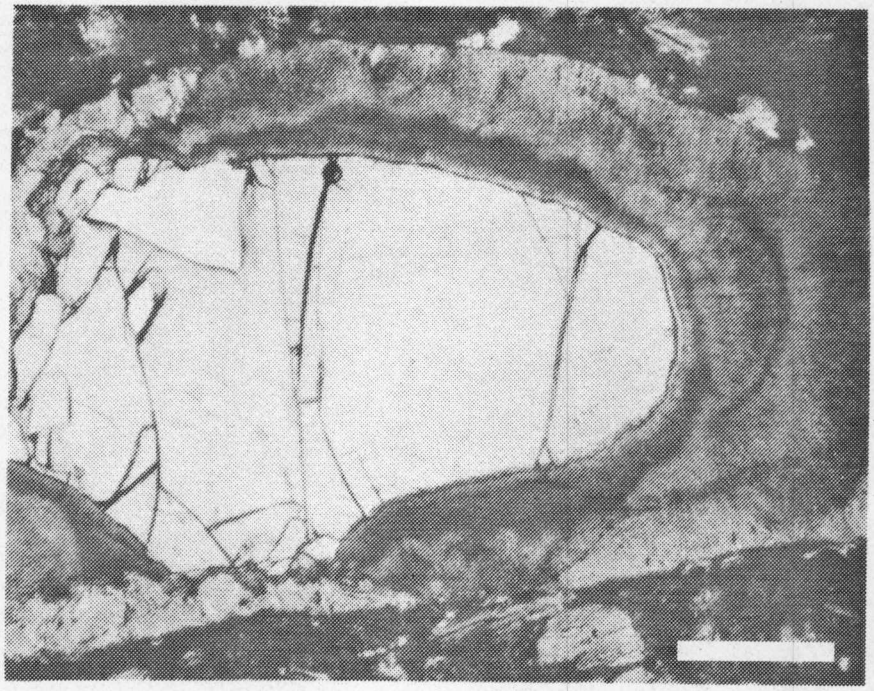

a

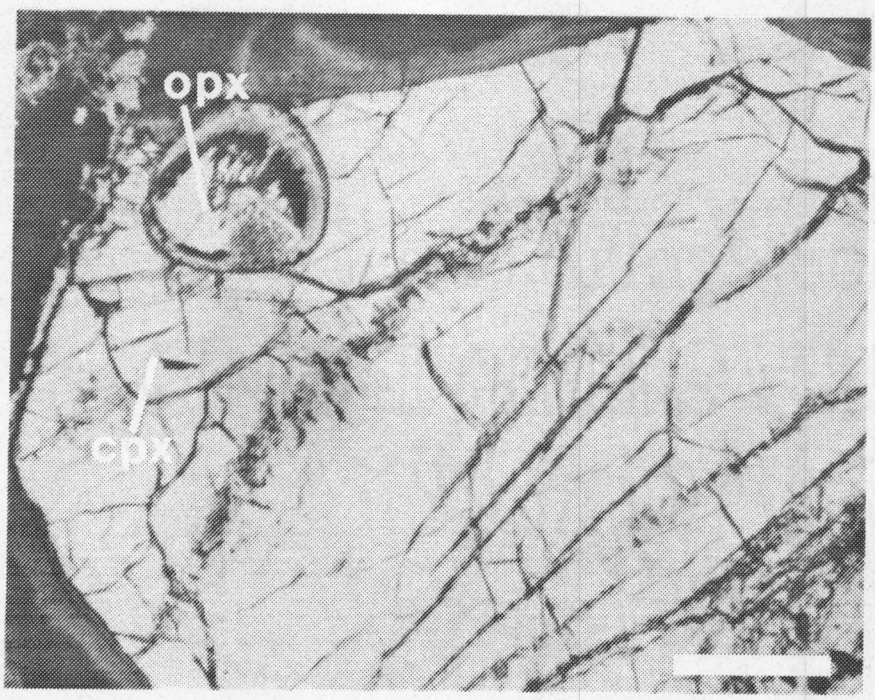

b

Figure 3.

Figure 4. Transmitted-light photomicrograph of clinopyroxene. Scale bar = 500 μm.

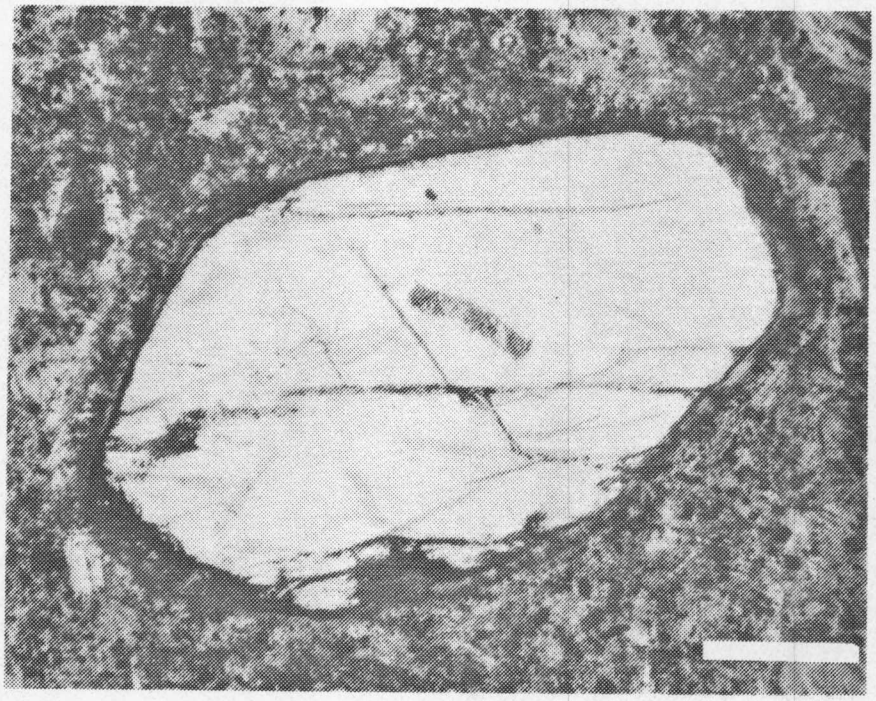

Figure 4.

have been observed in some megacrysts. Occurrences of orthopyroxene are limited to a few partially altered megacrysts (0.08 - 0.2 cm in diameter) and to rare inclusions in garnet and serpentinized olivine. Alteration to serpentine and other hydrous silicates is well advanced, especially along margins, fractures and cleavages. Reaction rims, if present originally, have been obscured or obliterated by alteration products.

Phlogopite is present as rounded crystals (up to 0.12 cm in size), smaller, euhedral groundmass grains (Figure 5), and as a reaction product forming mantles on some clinopyroxene megacrysts and kelyphitic rims on surrounding garnets. Many of the larger crystals exhibit optical zonation. Spinel inclusions have been observed in the outer margins of these large grains and in the cores of some groundmass crystals. Phlogopites typically show chlorite alteration along grain margins and fractures.

Several types of oxide minerals are present, of which spinels represent the most abundant. Spinel megacrysts are typically ovoid, translucent, and reddish-brown in color, although a green variety is also present (Figure 6). Megacrysts may exhibit one or both of the following reaction rims: (1) pale-blue, Cr-spinel; (2) brown, Ti-magnetite (rim widths average 60 - 100 μm). If both rims are present on a single megacryst, the paragenetic sequence of Cr-spinel followed by Ti-magnetite is observed. Cr-spinel and Ti-magnetite are present also as small (15 - 50 μm) euhedral grains in the groundmass. Although both minerals occur as discrete grains, they can be associated in the form of a Cr-spinel core surrounded by a discrete Ti-magnetite

Figure 5. Transmitted-light photomicrograph of phlogopite laths oriented in a trachytic-like texture. Note kinking and shredding of laths. Scale bar = 500 μm.

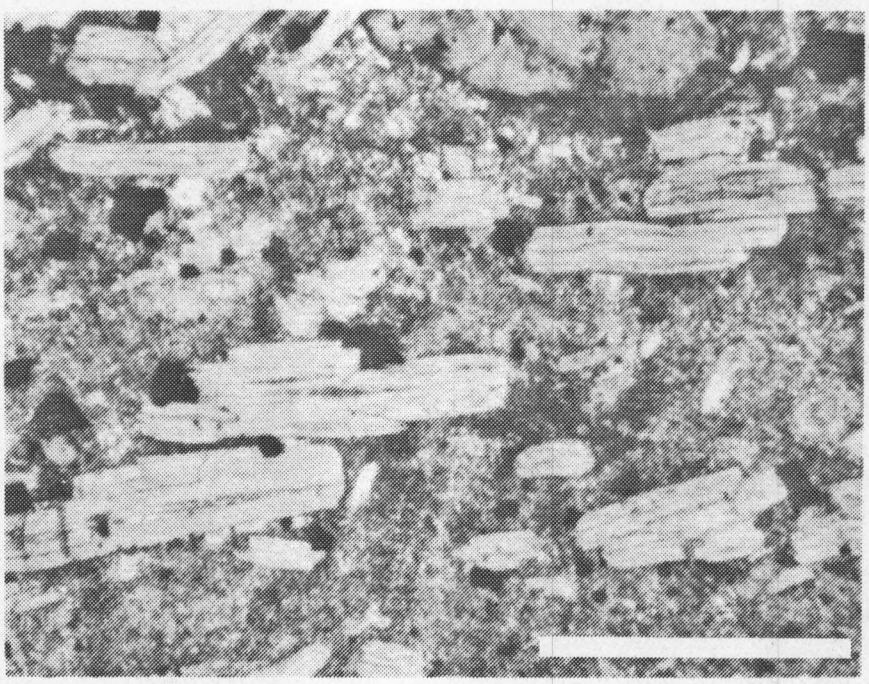

Figure 5.

Figure 6. Transmitted-light photomicrographs of spinel megacrysts. Scale bar = 250 μm.

a. Green spinel rimmed by phlogopite.

b. Brown spinel rimmed by Ti-magnetite.

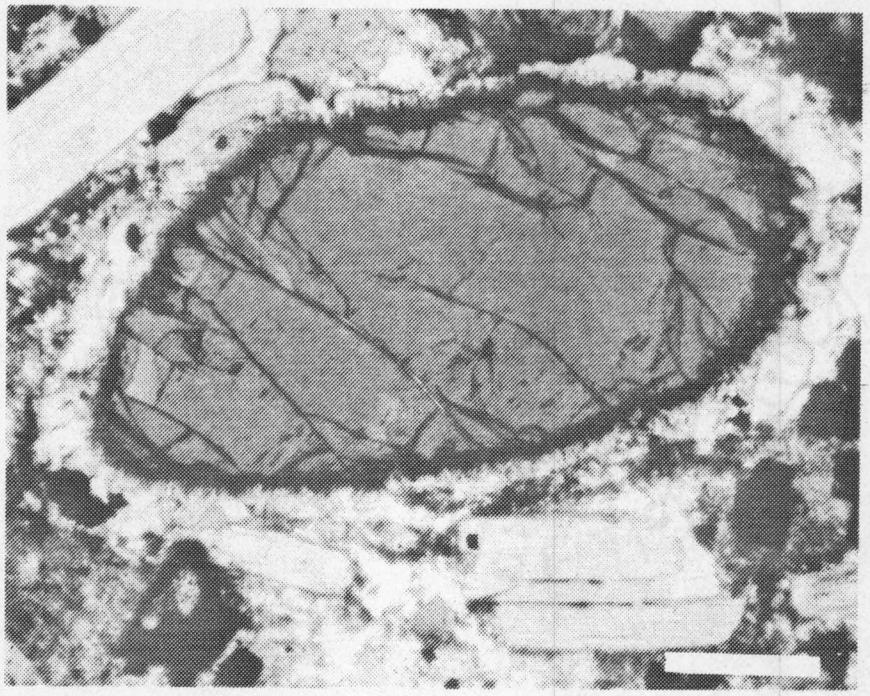

a

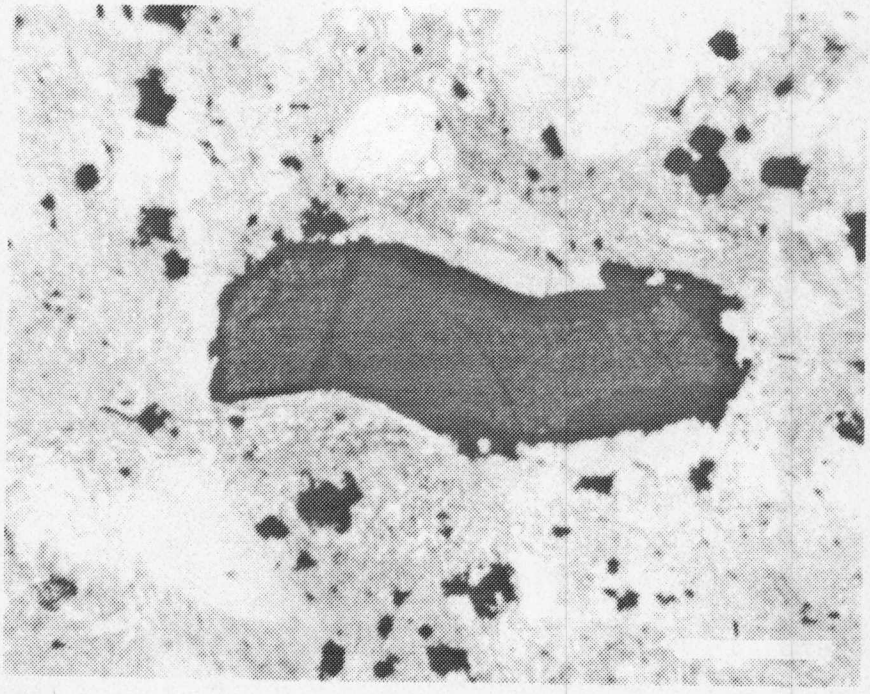

b

Figure 6.

rim (Figure 7a); skeletal or atoll morphologies are exhibited by many of the grains (Figure 7b). Perovskite is disseminated throughout the groundmass as discrete anhedra (10 - 40 μm) and also occurs as a reaction product rimming Ti-magnetite. Both of these textural types commonly occur as aggregates of microcrystalline grains. Rutile occurs as rounded groundmass grains (10 - 30 μm), as acicular inclusions in clinopyroxene megacrysts, and as an accessory in eclogite. Rare ilmenite grains (up to 50 μm in size) occur in association with Cr-spinel.

Sulfides (pyrrhotite, chalcopyrite, and pentlandite) occur throughout the groundmass as small (10 - 20 μm), subhedral grains. They are also present as large blebs (30 - 40 μm) in some serpentinized olivine megacrysts.

Calcite occurs as the most abundant matrix constituent and, in some dikes, is the modally predominant mineral. Although it is generally disseminated throughout the matrix as minute crystals; irregular-shaped, aggregate concentrations of calcite have been noted in some samples. Calcite also occurs as an accessory mineral in serpentinized olivine megacrysts and forms rims (50 - 100 μm wide) around shale xenoliths.

Three types of xenoliths are present: (1) shale clasts; (2) eclogite nodules (Figure 8a); (3) spinel peridotite nodules (Figure 8b). The shale xenoliths are highly brecciated and are irregular in form. They typically are elongate (up to 6 cm long and 4 cm wide) and are most abundant near dike - country rock contacts. Some clasts are mantled by calcite and transected by calcite veinlets. Except for a darkened color around margins of some clasts, little effects of thermal alteration have been observed.

Figure 7. Transmitted-light photomicrographs of groundmass spinels. Scale bar = 30 μm.

a. Cr-spinel (cr) rimmed by Ti-magnetite (tmt). Perovskite (pk) mantles Ti-magnetite.

b. Cr-spinel (cr) mantled by Ti-magnetite (tmt). Perovskite (pk) forms reaction rim on Ti-magnetite. Note skeletal morphology.

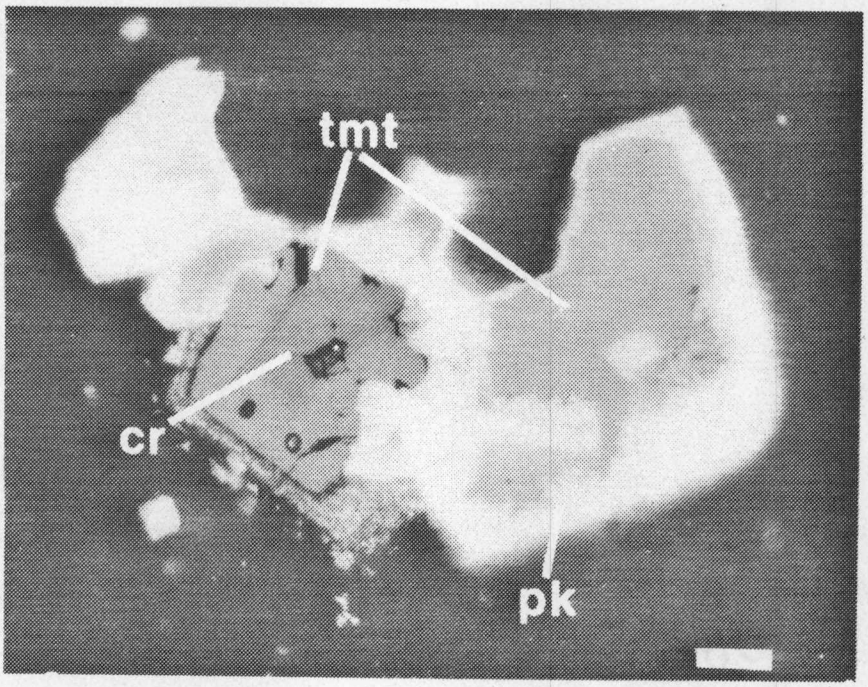

a

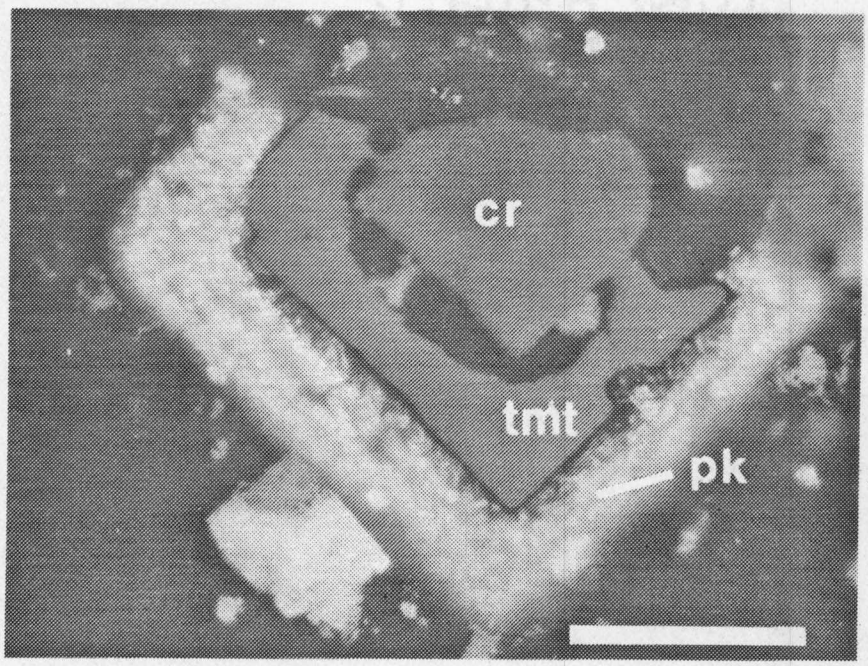

b

Figure 7.

Figure 8. Transmitted-light photomicrographs of ultramafic xenoliths. Scale bar = 500 μm.

a. Eclogite nodule comprising intergrowths of clinopryoxene (cpx) and garnet (gt). Plagioclase (pl) is present as an accessory.

b. Spinel peridotite nodule consisting of serpentinized olivine (s ol), brown, Cr-Al spinel (sp), and clinopyroxene (cpx).

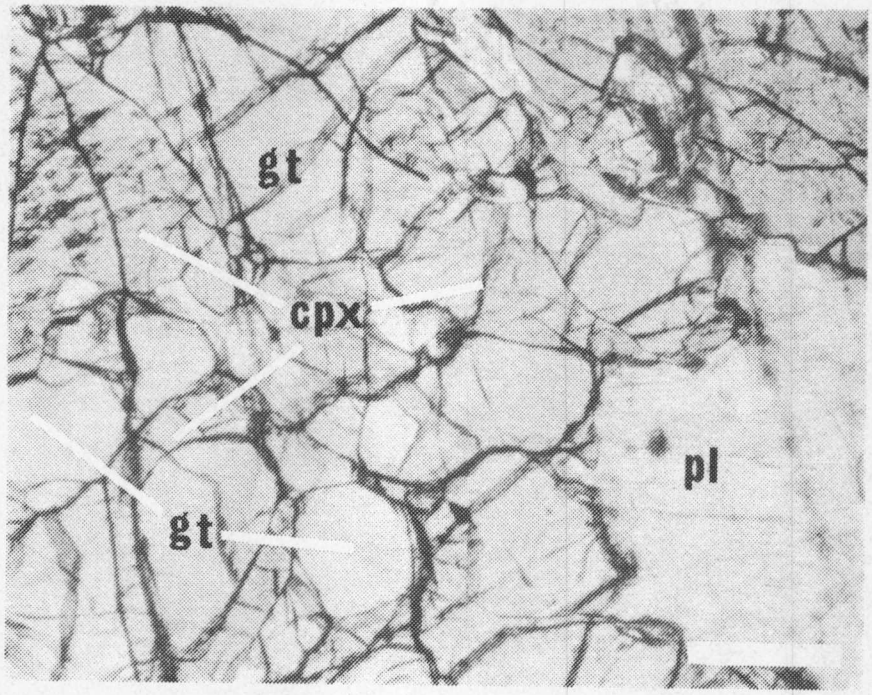

a

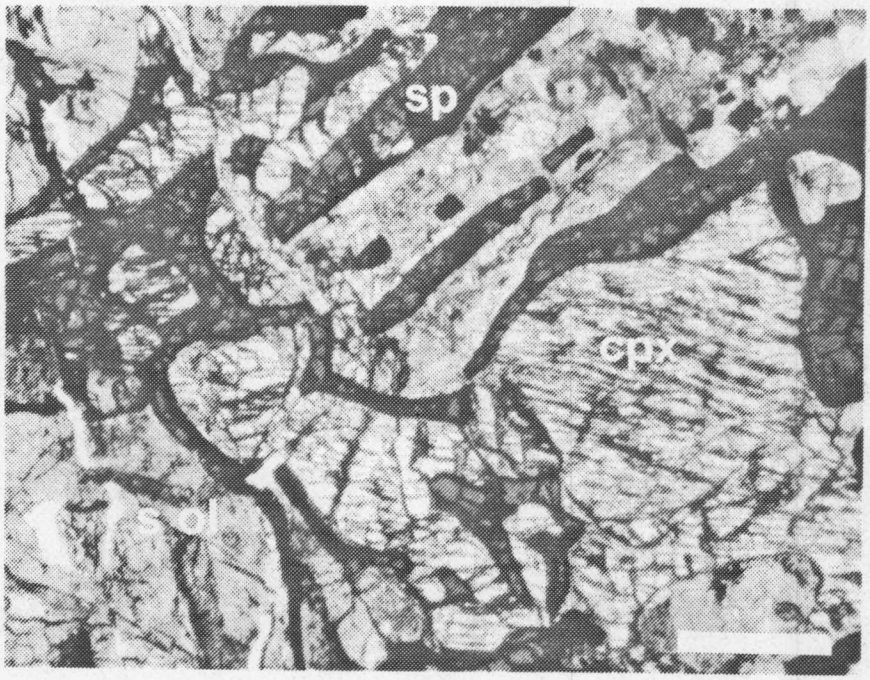

b

Figure 8.

Eclogite xenoliths occur as irregular-shaped, rounded nodules up to 1 cm in diameter. The nodules consist of graphic intergrowths (up to 0.10 cm wide) of garnet and clinopyroxene. Grain boundaries between these phases are sharp and well-defined, exhibiting no evidence of alteration. The clinopyroxene is distinctly green in color and displays faint pleochroism. Garnet in eclogite lacks kelyphitic alteration along grain boundaries within xenoliths; however, some kelyphitic rims have developed around the external margins of garnets in contact with the groundmass. Minor amounts of plagioclase occur in two textural forms: (1) as interstitial material (up to 0.10 cm in size) between clinopyroxene and garnet; (2) as rounded inclusions (0.02 - 0.06 cm in size) within clinopyroxene. Rutile is present as acicular inclusions in clinopyroxenes and as interstitial inclusions between garnet and clinopyroxene.

Spinel peridotite xenoliths, up to 1.5 cm in size, also occur as rounded, irregular-shaped nodules. These xenoliths consist primarily of serpentinized olivine with lesser amounts of clinopyroxene, translucent, brown spinel, and entirely serpentinized orthopyroxene. Clinopyroxene and altered orthopyroxene are present interstitially to serpentinized olivine. Spinel occurs as elongate inclusions (0.05 - 0.10 cm long) in serpentized olivine; these spinels are optically similar to spinel megacrysts.

CHAPTER III

MINERAL CHEMISTRY

On the basis of Cr-contents, garnets and clinopyroxenes can be divided into two populations: Group I (Cr-rich), or Group II (Cr-poor); the maximum Cr-contents in both of these groups is less than those which typically define Cr-rich and Cr-poor megacryst suites observed from other kimberlites (e.g., Colorado/Wyoming, Eggler et al., 1979). Representative analyses of Group I and Group II garnets and clinopyroxenes are presented in Tables 1 and 2.

Group I. Group I garnets are distinguished by a range of Cr_2O_3 contents (0.20 - 3.97%) and restricted mg (0.75 - 0.84); clinopyroxenes contain 0.76 to 1.47% Cr_2O_3 and possess mg values ranging from 0.91 to 0.95 (Figure 9.). Clinopyroxenes occurring in spinel peridotite xenoliths fall within this compositional range. Enstatite compositions (Table 3) also possess restricted mg (0.90 - 0.92) and a high range of Cr-contents (0.26 - 0.63% Cr_2O_3).

Figure 10 shows the compositional relationships between enstatite and Group I garnets and clinopyroxenes; tie lines connecting these fields are typical for kimberlite mineral relationships. The evidence that these three phases are cogenetic rests in the high Cr_2O_3 and high mg common to this suite, and in petrographic evidence in the form of enstatite and diopside inclusions within pyrope.

Spinel megacrysts, the fourth Group I component, contain less than 0.2% TiO_2 and variable Cr/Cr + Al (0.01 - 0.79), thus distinguishing

Table 1. Representative electron microprobe analyses of garnet.

	GROUP I				GROUP II			
								(eclogite)
SiO_2	41.9 (3)*	41.9 (5)	42.2 (6)	42.1 (3)**	41.3 (2)	40.1 (1)	39.7 (5)	38.8 (4)
TiO_2	0.05(1)	0.21(1)	0.19(1)	0.17(2)	0.07(2)	0.15(2)	0.11(2)	0.08(1)
Al_2O_3	19.7 (6)	21.6 (4)	23.5 (2)	21.7 (2)	22.1 (3)	22.6 (2)	21.1 (2)	21.8 (7)
Cr_2O_3	3.97(15)	1.75(7)	0.20(3)	2.25(6)	0.02(1)	0.04(3)	0.03(2)	0.03(1)
MgO	20.3 (3)	20.0 (2)	22.3 (1)	20.2 (1)	15.0 (2)	12.9 (1)	9.80(11)	10.6 (1)
FeO	7.61(17)	8.93(9)	7.84(13)	8.39(8)	16.3 (2)	18.3 (2)	23.6 (3)	22.7 (1)
MnO	0.41(4)	0.42(1)	0.24(4)	0.46(4)	0.49(2)	0.54(5)	0.50(3)	0.58(5)
CaO	5.91(6)	5.08(7)	4.20(6)	5.13(4)	5.31(6)	5.34(4)	5.46(7)	5.53(3)
Total	99.85	99.89	100.67	100.40	100.59	99.97	100.30	100.12
	Cations on the basis of 12 oxygens							
Si	3.014	3.001	2.961	3.000	3.017	2.982	3.024	2.956
Ti	0.002	0.010	0.008	0.008	0.002	0.006	0.004	0.004
Al	1.666	1.818	1.941	1.821	1.907	1.986	1.895	1.962
Cr	0.224	0.099	0.010	0.125	0.006	0.002	0.001	0.001
Mg	2.179	2.137	2.331	2.139	1.637	1.427	1.114	1.200
Fe	0.458	0.534	0.459	0.499	0.993	1.136	1.501	1.477
Mn	0.023	0.025	0.012	0.027	0.030	0.033	0.031	0.036
Ca	0.454	0.389	0.315	0.391	0.416	0.424	0.445	0.450
Σ	8.020	8.013	8.037	8.010	8.008	7.996	8.014	8.055

* Units in ( ) represent one standard deviation of replicate analyses in terms of least units cited.

** Garnet megacryst contains inclusions of cpx and opx.

Table 2. Representative electron microprobe analyses of clinopyroxene.

	GROUP I			GROUP II				
	megacryst	megacryst	inclusion in garnet	megacryst	megacryst	megacryst core	megacryst rim	eclogite
SiO_2	52.7 (4)*	53.5 (10)	54.6 (3)	50.4 (4)	52.5 (5)	47.2 (3)	52.9 (4)	50.9 (3)
TiO_2	0.51(3)	0.48(2)	0.28(2)	0.69(8)	0.86(3)	1.16(5)	0.81(8)	0.89(20)
Al_2O_3	4.42(6)	4.05(13)	2.55(4)	7.24(21)	1.57(11)	11.6 (1)	1.50(26)	6.81(42)
Cr_2O_3	1.47(4)	0.76(4)	1.38(7)	n.d.**	n.d.	n.d.	0.25(9)	0.05(4)
MgO	15.4 (1)	15.6 (4)	16.0 (2)	11.3 (1)	16.7 (1)	12.0 (2)	16.4 (2)	11.3 (3)
FeO	1.95(8)	2.53(23)	2.18(8)	8.32(23)	4.61(31)	6.16(26)	4.19(23)	7.79(61)
MnO	0.04(4)	0.06(3)	n.d.	0.18(5)	0.09(4)	0.11(3)	0.13(5)	0.07(3)
CaO	20.7 (3)	19.6 (3)	20.9 (1)	19.5 (2)	22.4 (2)	20.4 (7)	22.5 (3)	19.3 (4)
Na_2O	2.13(5)	2.38(16)	1.60(1)	1.80(3)	0.65(8)	1.11(9)	0.58(10)	2.54(9)
Total	99.32	98.96	99.49	99.43	99.38	99.74	99.26	99.65
	Cations on the basis of 6 oxygens							
Si	1.921	1.952	1.979	1.873	1.938	1.738	1.950	1.885
Ti	0.014	0.013	0.007	0.018	0.023	0.031	0.022	0.024
Al	0.189	0.173	0.108	0.316	0.068	0.505	0.064	0.297
Cr	0.042	0.021	0.039	---	---	---	0.006	0.001
Mg	0.834	0.847	0.866	0.628	0.917	0.658	0.902	0.625
Fe	0.059	0.077	0.066	0.258	0.142	0.189	0.129	0.241
Mn	0.001	0.001	---	0.005	0.002	0.003	0.003	0.001
Ca	0.806	0.766	0.809	0.777	0.884	0.803	0.889	0.768
Na	0.149	0.167	0.111	0.129	0.046	0.079	0.041	0.182
Σ	4.015	4.017	3.985	4.004	4.020	4.006	4.006	4.024

* Units in ( ) represent one standard deviation of replicate analyses in terms of least units cited.

** n.d. = not detected.

Figure 9. Cr_2O_3 (wt. %) vs. Mg/Mg + Fe^{2+} for garnets and clinopyroxenes in the Taughannock Creek kimberlite.

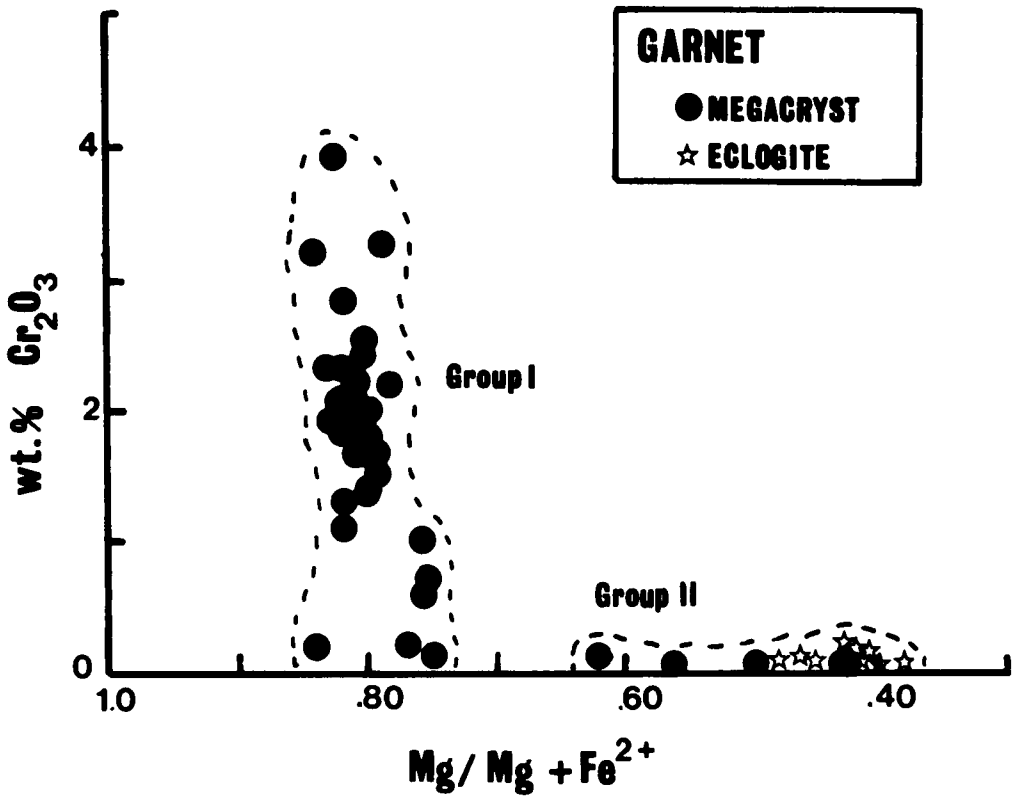
GARNET
MEGACRYST
ECLOGITE
wt.% Cr_2O_3
4
2
0
Group I
Group II
1.0
.80
.60
.40
$Mg/Mg+Fe^{2+}$

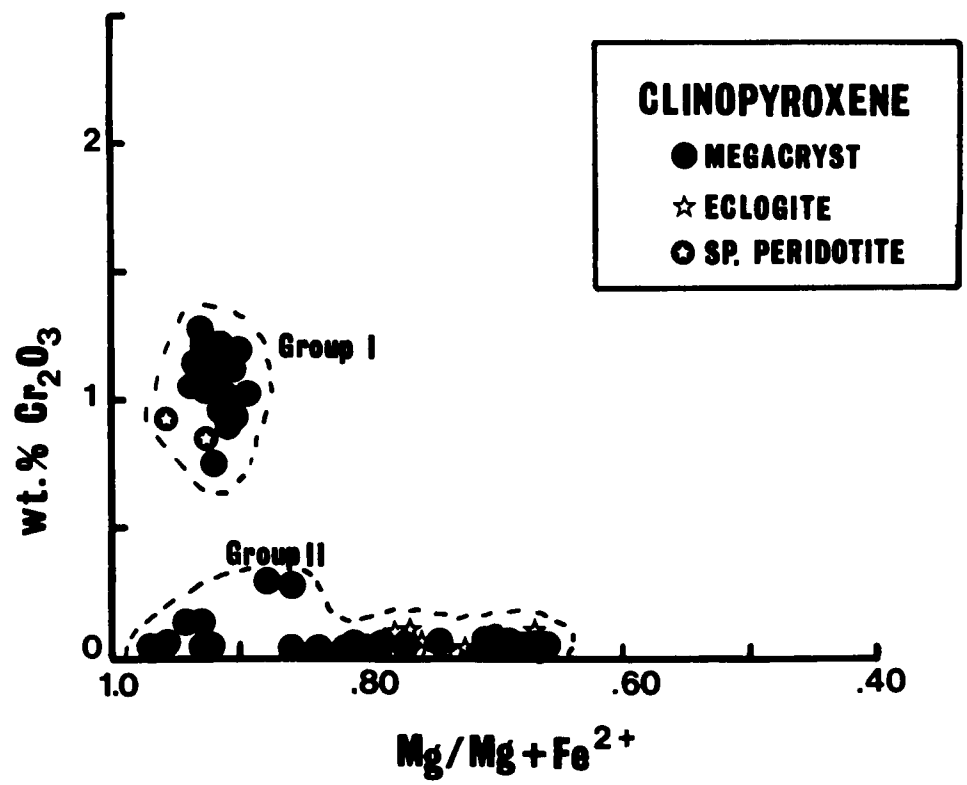
CLINOPYROXENE
MEGACRYST
ECLOGITE
SP. PERIDOTITE
wt.% Cr_2O_3
2
1
0
Group I
Group II
1.0
.80
.60
.40
$Mg/Mg+Fe^{2+}$

Figure 9.

Table 3. Representative electron microprobe analyses of orthopyroxene.

	megacryst	megacryst	megacryst	megacryst	inclusion in garnet
SiO_2	55.5 (4)*	57.5 (9)	56.3 (1)	54.6 (3)	57.4 (7)
TiO_2	0.11(1)	0.07(1)	0.05(2)	0.15(5)	0.11(2)
Al_2O_3	1.14(4)	2.66(8)	3.38(15)	4.95(9)	1.11(6)
Cr_2O_3	0.26(3)	0.55(3)	0.63(10)	0.38(4)	0.30(1)
MgO	36.0 (3)	32.3 (9)	33.4 (3)	33.2 (5)	34.8 (2)
FeO	5.59(9)	4.98(6)	5.44(9)	6.57(20)	5.35(14)
MnO	0.09(3)	0.17(3)	0.11(5)	0.11(1)	0.09(1)
CaO	0.38(1)	0.66(4)	0.49(8)	0.59(4)	0.29(1)
Na_2O	n.d.**	0.04(4)	0.03(1)	0.08(1)	0.04(1)
Total	99.07	98.93	99.83	100.63	100.30
		Cations on the basis of 6 oxygens			
Si	1.933	1.986	1.936	1.876	1.979
Ti	0.002	0.001	0.001	0.003	0.002
Al	0.046	0.107	0.136	0.200	0.044
Cr	0.006	0.014	0.016	0.010	0.008
Mg	1.870	1.666	1.712	1.701	1.789
Fe	0.163	0.144	0.155	0.188	0.153
Mn	0.002	0.004	0.003	0.003	0.002
Ca	0.013	0.024	0.017	0.021	0.010
Na	---	0.002	0.001	0.005	0.002
Σ	4.035	3.948	3.997	4.007	3.989

* Units in ( ) represent one standard deviation of replicate analyses in terms of least units cited.
** n.d.= not detected.

Figure 10. Ternary plot of atomic Ca-Mg-Fe for Group I garnets, clinopyroxenes and orthopyroxenes. Outlined fields represent Cr-rich compositions of minerals from Colorado/ Wyoming kimberlites (Eggler, 1979).

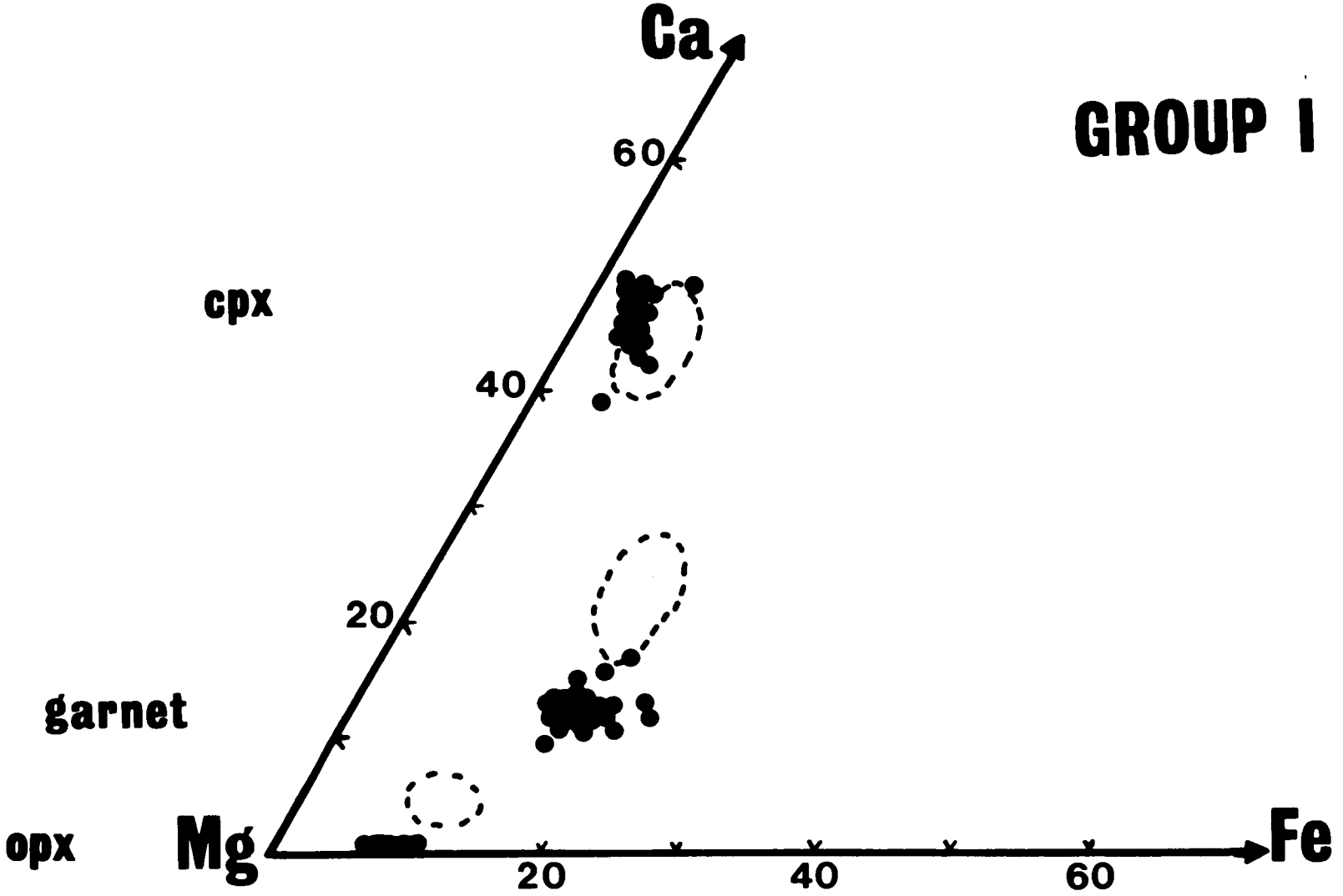

Figure 10.

them significantly from the groundmass spinels (Figure 11). Spinels in peridotite xenoliths also fall within the compositional range of the megacrysts (Table 4). These compositions are similar to those reported from megacrysts, as well as from spinel peridotite constituents from the upper mantle (e.g., Clarke and Mitchell, 1975; Boyd and Nixon, 1975; Smith and Dawson, 1975).

Group I garnets and clinopyroxenes have mg and Cr_2O_3 values similar to those reported from the Monastery kimberlite (Gurney et al., 1979) and the Cr-poor suite of the Colorado/Wyoming kimberlites (e.g., Eggler et al., 1979). In addition, the Group I megacrysts fall within the compositional range of megacrysts reported from other eastern United States occurrences (e.g., Garrison and Taylor, 1980), and are similar to those phases occurring in a Cr-bearing, garnet peridotite suite reported from Michigan (e.g., McGee and Hearn, 1982).

Group II. In comparison with the Group I assemblage, Group II minerals possess lower Cr_2O_3 values and exhibit a wider variation in mg (garnets, $\leq$ 0.04% Cr_2O_3: mg = 0.38 - 0.62; clinopyroxene, $\leq$ 0.32% Cr_2O_3: mg = 0.66 - 0.97). Compositional relationships between garnets and clinopyroxenes of this Group are shown in Figure 12. These phases, occurring in various textural intergrowths (nodular eclogite and garnet inclusions in clinopyroxene megacrysts), have compositions indistinguishable from those phases occurring as Group II megacrysts. This identity of chemical compositions implies a cogenetic relationship. Compositionally, these phases resemble eclogite assemblages reported from other kimberlite occurrences (e.g., Griffin et al., 1979; Snedden and Kay, 1981b; Schulze and Helmstaedt, 1978). Variability of minor

Figure 11. Spinel compositions plotted in 2Ti-Cr-Al ternary. Relationship to spinel prism is shown in inset. Tie lines indicate core-rim relationships.

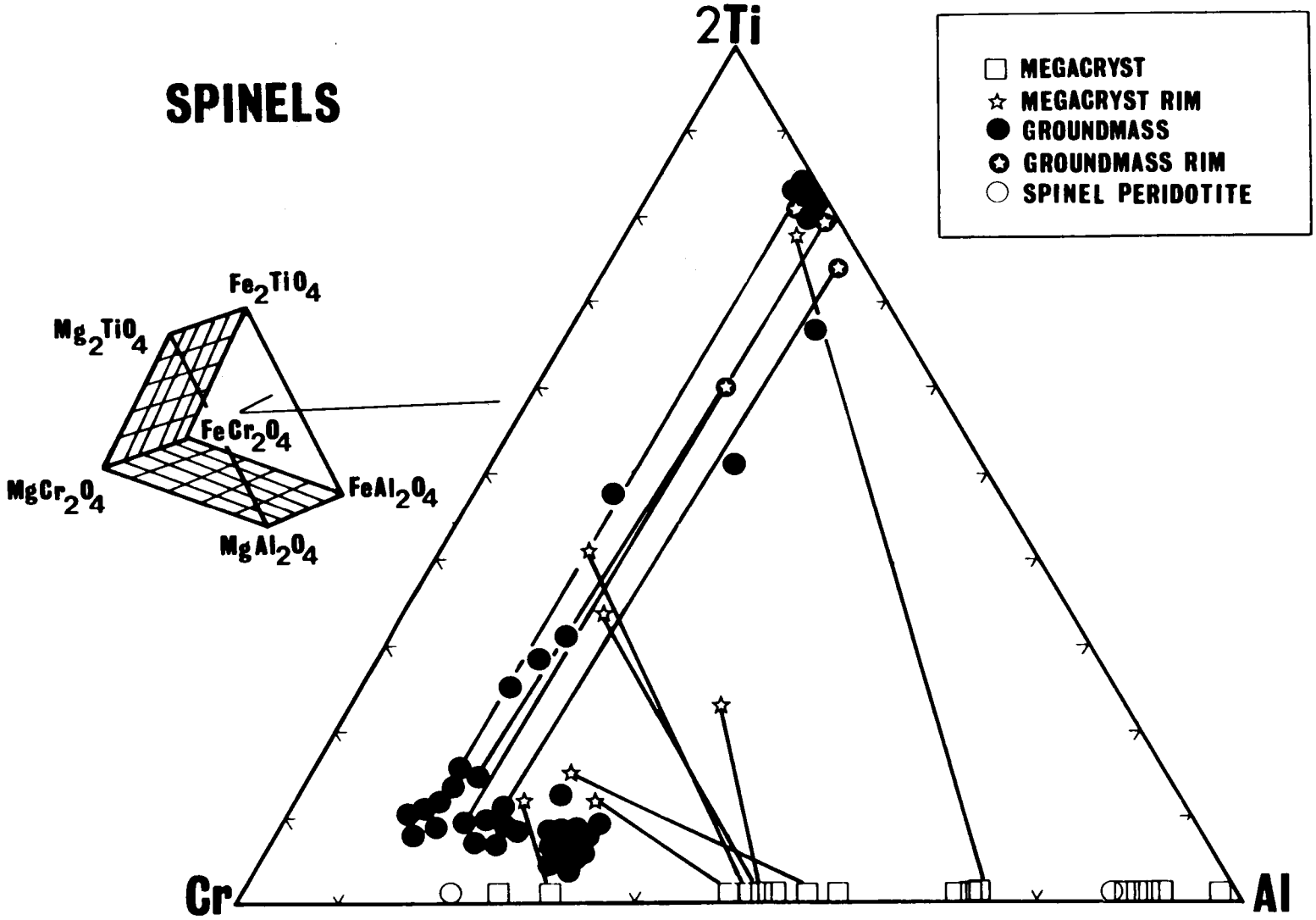
SPINELS
2Ti
Cr
Al
MEGACRYST
MEGACRYST RIM
GROUNDMASS
GROUNDMASS RIM
SPINEL PERIDOTITE
Fe_2TiO_4
Mg_2TiO_4
$FeCr_2O_4$
$MgCr_2O_4$
$FeAl_2O_4$
$MgAl_2O_4$

Figure 11.

Table 4. Representative electron microprobe analyses of spinel.

	megacryst	megacryst	megacryst		megacryst		spinel	spinel
			core	rim	core	rim	peridotite	peridotite
TiO_2	0.06(1)*	0.05(5)	0.19(1)	3.93(41)	0.16(2)	15.1 (5)	0.08(1)	0.09(1)
Al_2O_3	10.6 (1)	54.3 (5)	32.1 (3)	13.0 (4)	28.1 (2)	4.26(13)	42.7 (3)	54.8 (3)
Cr_2O_3	59.9 (9)	12.4 (2)	36.5 (5)	37.1 (14)	40.0 (5)	1.90(19)	25.0 (2)	11.8 (2)
Fe_2O_3**	5.39	2.02	1.93	15.0	2.21	37.3	1.74	2.07
MgO	15.5 (1)	19.1 (4)	16.0 (2)	13.6 (3)	14.3 (8)	9.75(30)	17.7 (2)	19.7 (2)
FeO	10.3 (2)	11.1 (2)	12.8 (1)	16.5 (9)	14.6 (2)	29.8 (15)	11.5 (1)	10.5 (2)
MnO	0.26(3)	0.16(3)	0.24(3)	0.41(5)	0.37(1)	0.80(10)	0.19(3)	0.20(3)
Total	101.11	99.13	99.76	99.54	99.74	98.91	98.91	99.16
			Cations on the basis of 4 oxygens					
Ti	0.001	0.001	0.004	0.095	0.004	0.395	0.002	0.002
Al	0.394	1.692	1.102	0.493	0.995	0.175	1.403	1.703
Cr	1.470	0.261	0.842	0.945	0.940	0.052	0.551	0.246
Fe^{3+}	0.128	0.040	0.042	0.363	0.050	0.979	0.037	0.041
Mg	0.730	0.755	0.693	0.652	0.638	0.507	0.736	0.773
Fe^{2+}	0.271	0.247	0.311	0.443	0.365	0.868	0.268	0.232
Mn	0.006	0.004	0.006	0.009	0.008	0.024	0.003	0.003
Σ	3.000	3.000	3.000	3.000	3.000	3.000	3.000	3.000

* Units in ( ) represent one standard deviation of replicate analyses in terms of least units cited.

** All Fe is determined as FeO; Fe^{3+} is calculated assuming stoichiometry.

Figure 12. Ternary plot of atomic Ca-Mg-Fe for Group II garnets and clinopyroxenes. Tie lines connect coexisting phases in eclogite.

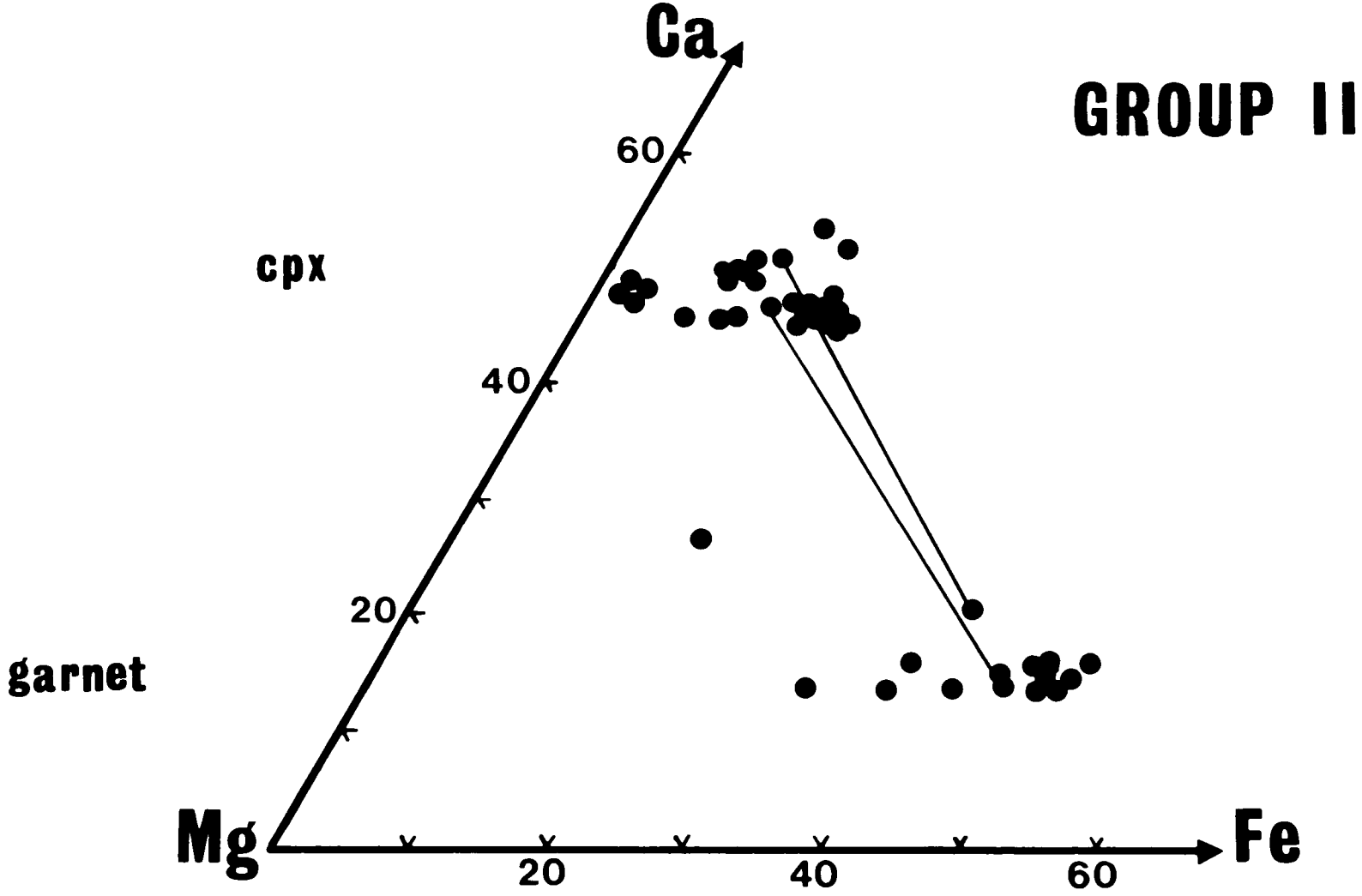

Figure 12.

components with mg show correlations that are interpreted to result from crystal fractionation within this group: Na_2O, Al_2O_3, and TiO_2 increase with increasing mg (Figure 13). In general, megacrysts in this suite lack chemical zonation; however, reverse core-rim zonation has been observed in a number of clinopyroxene megacrysts. Depletion in TiO_2 and Na_2O, and enrichment in MgO and Cr_2O_3 in the rims, suggests re-equilibration via the introduction of a more primitive magma into the Group II environment.

Groundmass Oxides. Representative groundmass oxide analyses are shown in Table 5. The groundmass spinels as a group possess a continuum of compositions from Cr-spinel (46.46% Cr_2O_3, 1.99% TiO_2) to Ti-magnetite (0.41% Cr_2O_3, 16.75% TiO_2). The progressive Ti-enrichment exhibited by these spinel compositions is characteristic of late-stage chemical trends within spinels occurring in kimberlite (e.g., Haggerty, 1976). The epitaxial rims occurring on spinel megacrysts correlate with various groundmass compositions. Rare groundmass ilmenite contains 10 to 12% MgO and 1.40 to 1.80% Cr_2O_3; these are similar to typical groundmass ilmenites in kimberlites (e.g., Pasteris, 1980). Perovskite analyses indicate the presence of minor amounts of FeO, Cr_2O_3, and Al_2O_3. Semi-quantitative energy dispersive techniques indicate that Nb and REE's are also present; perovskite in kimberlite can contain up to 10 wt. % REE's (Boctor and Meyer, 1970; Boctor and Boyd, 1980).

Representative phlogopite analyses are presented in Table 6. Compositional ranges are as follows: 21.36 - 24.08% MgO; 0.07 - 1.71% Cr_2O_3; 0.75 - 4.64% TiO_2; 12.47 - 14.80% Al_2O_3. These compositions are

Figure 13. Wt. % TiO_2, Al_2O_3 and Na_2O *vs.* Mg/Mg + Fe^{2+} for Group II clinopyroxenes. Tie lines connect core-rim analyses.

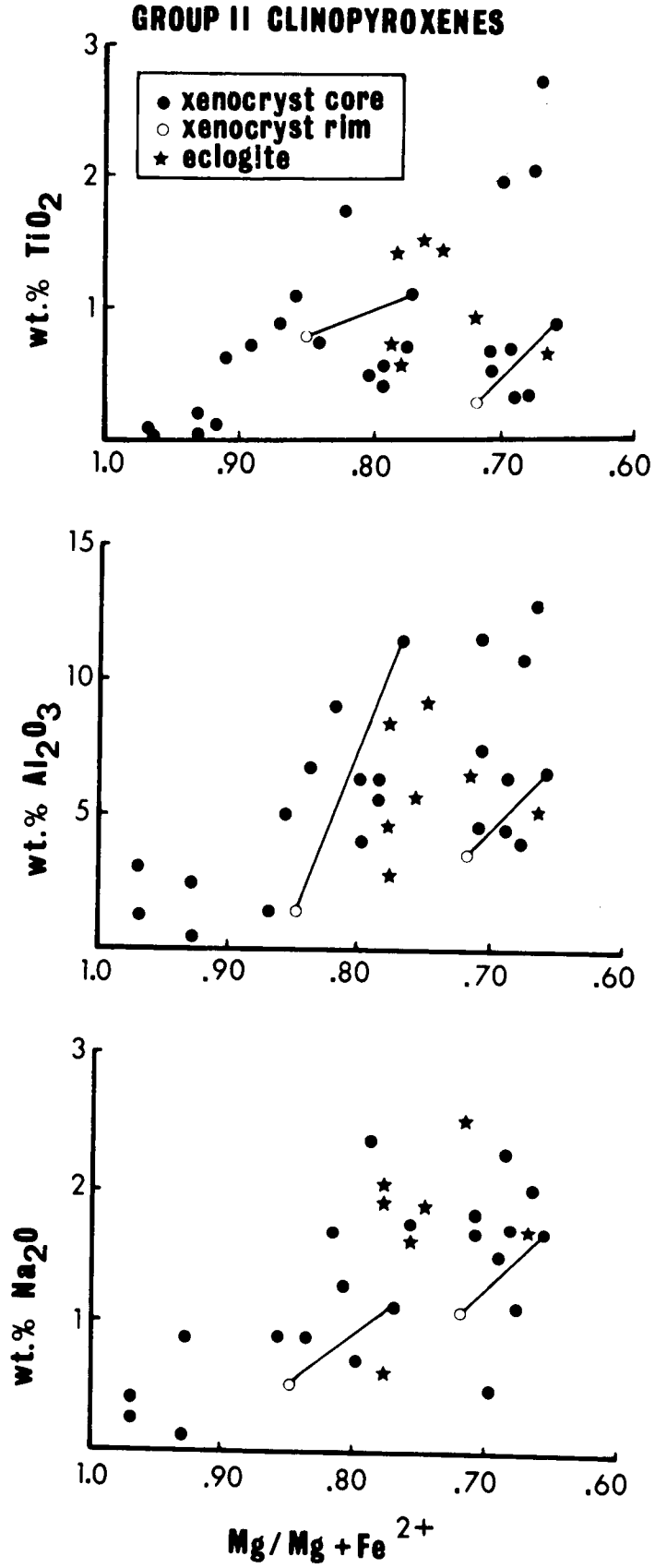
GROUP II CLINOPYROXENES
xenocryst core
xenocryst rim
eclogite
wt.% TiO2
wt.% Al2O3
wt.% Na2O
1.0
.90
.80
.70
.60
Mg/Mg + Fe 2+

Figure 13.

Table 5. Representative electron microprobe analyses of groundmass oxides.

	Cr-sp	Cr-sp	Cr-sp core	Cr-sp rim	Ti-mt	Ti-mt	Ilmenite	perovskite
TiO_2	2.55(30)*	9.51	2.29(5)	8.23	15.5 (2)	16.8	52.1 (10)	56.7 (3)
Al_2O_3	8.50(9)	5.79	15.1 (1)	3.34	4.40(2)	4.51	0.36(1)	0.22(1)
Cr_2O_3	49.6 (12)	8.81	44.2 (3)	5.31	0.11(4)	0.41	1.55(7)	0.24(4)
Fe_2O_3**	9.81	39.6	7.89	47.8	38.3	36.7	7.8	---
MgO	12.5 (1)	10.9	13.8 (1)	8.28	10.0 (1)	11.4	11.4 (3)	n.a.***
FeO	16.4 (5)	23.7	15.1 (2)	26.4	30.6 (5)	29.3	26.4 (6)	1.36(9)
MnO	0.33(3)	0.70	0.40(3)	0.47	0.65(4)	0.67	0.61(1)	n.a.
CaO	n.a.	n.a.	n.a.	n.a.	n.a.	n.a.	n.a.	38.9 (2)
Total	99.69	99.01	98.78	99.83	99.56	99.79	100.22	97.42****
Cation Basis	(4)	(4)	(4)	(4)	(4)	(4)	(3)	(3)
Ti	0.063	0.246	0.055	0.218	0.404	0.430	0.910	0.993
Al	0.330	0.234	0.570	0.134	0.179	0.182	0.010	0.005
Cr	1.292	0.239	1.118	0.148	0.003	0.010	0.028	0.004
Fe^{3+}	0.243	1.023	0.190	1.269	0.997	0.943	0.136	---
Mg	0.613	0.559	0.656	0.438	0.517	0.580	0.393	---
Fe^{2+}	0.451	0.682	0.403	0.778	0.884	0.836	0.512	0.026
Mn	0.008	0.017	0.009	0.015	0.016	0.019	0.011	---
Ca	---	---	---	---	---	---	---	0.971
Σ	3.000	3.000	3.000	3.000	3.000	3.000	2.000	1.999

* Units in ( ) represent one standard deviation of replicate analyses in terms of least units cited. ** All Fe is determined as FeO; Fe^{3+} is calculated assuming stoichiometry.
*** n.a.= not analyzed. **** Low total due to the presence of Nb and REEs.

Table 6. Representative electron microprobe analyses of phlogopite.

	xenocryst		xenocryst		groundmass
	core	rim	core	rim	
SiO_2	39.2 (9)*	39.2 (7)	40.9 (3)	37.8 (4)	37.7 (4)
TiO_2	0.75(1)	1.82(5)	0.90(3)	3.29(7)	3.46(2)
Al_2O_3	13.7 (1)	14.2 (7)	12.5 (13)	14.7 (1)	14.8 (2)
Cr_2O_3	0.67(3)	1.07(12)	0.61(6)	1.71(31)	1.56(12)
MgO	23.5 (5)	23.2 (2)	24.1 (1)	22.5 (3)	22.0 (5)
FeO	4.45(6)	4.41(21)	5.05(8)	4.93(18)	4.87(9)
MnO	0.08(6)	0.04(4)	0.10(3)	0.12(1)	0.09(3)
CaO	0.43(12)	n.d.**	n.d.	n.d.	n.d.
Na_2O	0.57(4)	0.74(14)	0.28(3)	0.36(3)	0.36(4)
K_2O	9.58(16)	9.25(6)	10.1 (1)	9.60(28)	9.80(2)
Total	92.93	93.96	94.54	95.01	94.64
		Cations on the basis of 22 oxygens			
Si	5.730	5.661	5.884	5.464	5.450
Ti	0.081	0.194	0.097	0.356	0.373
Al	2.357	2.405	2.112	2.500	2.521
Cr	0.077	0.118	0.067	0.131	0.178
Mg	5.117	4.996	5.116	4.849	4.750
Fe	0.540	0.529	0.604	0.593	0.585
Mn	0.008	0.004	0.008	0.013	0.008
Ca	0.064	---	---	---	---
Na	0.158	0.207	0.076	0.102	0.097
K	1.783	1.702	1.846	1.768	1.808
Σ	15.915	15.816	15.860	15.776	15.770

* All units in ( ) represent one standard deviation of replicate analyses in terms of least units cited.

** n.d. = not detected.

similar to those reported for phlogopite in kimberlite from Elliot Co., Kentucky (Garrison and Taylor, 1980) and Fayette Co., Pennsylvania (Hunter and Taylor, 1982b). They generally fall within the Type II kimberlite groundmass phlogopites of Smith et al., 1978. The larger phlogopite crystals are zoned from core to rim, with the rims showing increases in Cr_2O_3, TiO_2, and Al_2O_3, and a decrease in MgO; these rims exhibit compositional similarities with smaller (groundmass) phlogopites.

MgO contents in calcite range up to 0.42%; FeO ranges from 0.03 to 0.12%. These compositions are similar to those reported for calcite in kimberlite from South Africa (Smith et al., 1978).

CHAPTER IV

GEOTHERMOMETRY AND GEOBAROMETRY

Estimations of temperatures and pressures of equilibration of various mineral assemblages in these rocks rely on an evaluation and use of several different thermometers and barometers. The co-existence of a Ca-rich and Ca-poor pyroxene in the Group I suite permits the use of the experimentally determined diospide-enstatite solvus of Lindsley and Dixon (1976), the calculated solvus of Lindsley et al. (1981) and Lindsley (1980), and the empirical enstatite solvus of Boyd and Nixon (1973). Temperatures can also be calculated from Mg/Fe exchange between clinopyroxene and garnet using the equation in Gurney et al. (1979) fitted to the data of Akella and Boyd (1974); these data (Akella and Boyd, 1974) also enable the estimation of equilibration temperatures within the Group II eclogite assemblage.

Temperature estimates from Group I clinopyroxenes range from 950 - 1350° C (Table 7). These values were obtained using the 20 kb solvus of Lindsley and Dixon (1980) and the 30 kb solvus of Lindsley (1980). No appreciable differences were observed in the lower temperature range because the diopside limb is steep at both pressures. However, at higher temperatures a disparity of up to 50° C occurs, with the 30 kb solvus giving the higher values. Temperatures determined for the orthopyroxenes from the empirical Boyd and Nixon (1973) solvus range from 950 - 1110° C. Because the solubility of enstatite in clinopyroxene is reduced by increased amounts of Al_2O_3, unreliably low temperatures may result if the calculations are based

Table 7. Summary of geothermobarometric estimates.

	(1) T^{Di-En}_{cpx} (°C)	(2) T^{Di-En}_{cpx} (°C)	(3) T^{Di-En}_{cpx} (°C)	(4) T^{cpx-ga} (°C)	(5) $P^{Al_2O_3}_{opx}$ (kb)
Group I megacrysts	950-1300	950-1350	950-1110		25-31*
Group I inclusions	950	950	950	1005	
Group II megacrysts				716-1067	
Eclogite				950	

(1) Using the 20 kb Di-En solvus of Lindsley and Dixon (1976)
(2) Using the calculated 30 kb solvus of Lindsley (1980)
(3) Using the empirical enstatite solvus of Boyd and Nixon (1980)
(4) Using the data of Akella and Boyd (1974)
(5) Using the theoretical expression of Wood (1974), employing temperatures from (3)

* This range is calculated for orthopyroxenes with Al_2O_3 contents of less than 2.75%. Al_2O_3 contents and temperatures within two orthopyroxene megacrysts (3.83% Al_2O_3, 1050°C; 4.95% Al_2O_3, 1070°C) are consistent with equilibration in the spinel stability field (e.g. Perkins, et al., 1981) and are not included in this range.

on high-alumina pyroxenes. In view of this source of error, the majority of the temperature estimates were derived from pyroxenes containing less than 3% Al_2O_3. However, temperatures obtained using pyroxenes with greater than this amount (e.g., 4.95%) are within the overall ranges observed. Calculation of equilibration temperature of a clinopyroxene inclusion in a Group I garnet (which also contains an orthopyroxene inclusion) using the Mg/Fe exchange thermometer (e.g., Akella and Boyd, 1974; Gurney et al., 1979) returned a value of 1005° C, in reasonable agreement with the temperature estimated from the pyroxene inclusions (i.e., 950° C; Table 7).

Within the garnet stability field, Al_2O_3 content of orthopyroxene coexisting with garnet is a function of both temperature and pressure (e.g., MacGregor, 1974). Given a temperature and alumina content in orthopyroxene, an equilibration pressure can be calculated from the orthopyroxene megacrysts and inclusions using the theoretical expression of Wood (1974), although values obtained by this method may be overestimated (Perkins et al., 1981). For the purposes of calculation, the composition of the garnet containing the orthopyroxene inclusion was used (Ca/Ca + Mg + Fe = 0.129; Cr/Cr + Al = 0.064); temperatures were those obtained from the Boyd and Nixon (1973) solvus. Measured Al_2O_3 contents in the orthopyroxenes range from 1.11 to 4.95%. Two high-alumina orthopyroxene megacrysts (3.83 and 4.95% Al_2O_3) give temperatures of 1050° and 1070° C. On the basis of these alumina contents and temperatures, together with the phase relationships in the system MgO-Al_2O_3-SiO_2 it is concluded that these megacrysts crystallized within the spinel stability field (e.g.,

MacGregor, 1974; Perkins et al., 1981); in this region their Al_2O_3 contents are not pressure dependent. For the three orthopyroxenes with Al_2O_3 values between 2.66 and 1.11% the pressures obtained from the Wood (1974) expression range from 25 - 31 kb, corresponding to equilibration at depths between 75 and 95 km (i.e., within the garnet stability field).

The assemblage of Group I pyroxenes and garnets equilibrated over a temperature interval from 1350° C to 950° C, at depths ranging from 95 km to within the spinel stability field (40 - 70 km). The highest calculated pressure corresponds to a temperature of 1110° C; it is possible that the higher temperatures estimated from the clinopyroxenes are equivalent to a deeper source (assuming a typical geotherm). The P-T estimates derived from Group I megacrysts indicate that the crystallization interval for this suite spanned the garnet-spinel transition boundary; these results are corroborated by the petrographic observation of both garnet and spinel megacrysts within this assemblage.

The absence of orthopyroxene in the Group II assemblage precludes the use of the solvus thermometers and the possibility of calculating pressures from the expression of Wood (1974). Temperatures ranging from 717 to 1064° C were calculated from the Mg/Fe exchange between Group II garnets and clinopyroxenes (Akella and Boyd, 1974). These values were derived using K_D's calculated from various compositional pairs within the Group II megacryst population. The temperature calculated from the coexisting clinopyroxene and garnet in eclogite nodules is 950° C. The lower temperatures indicated by the megacrysts

undoubtedly reflect requilibration upon cooling. At the calculated temperatures quoted above, plagioclase and garnet can coexist at pressures ranging from 8 to 18 kb (Green and Ringwood, 1967); therefore, the presence of interstitial plagioclase in the eclogite nodules provides pressure constraints corresponding to a deep crustal/shallow upper mantle depth (25 to 50 km).

Figure 14 illustrates the P-T relationships estimated for Group I and Group II minerals. The depths of equilibration for these suites, as well as those inferred for kimberlitic assemblages from Fayette Co., Pennsylvania and Elliott Co., Kentucky, are plotted relative to the Lesotho geotherm.

Figure 14. Pressure (kb) - temperature (°C) - depth (km) relationships between Group I and Group II minerals from the Taughannock Creek kimberlite. Mineral assemblages in kimberlite from Fayette Co., Pennsylvania and Elliott Co., Kentucky are also shown. The Lesotho geotherm is shown for reference.

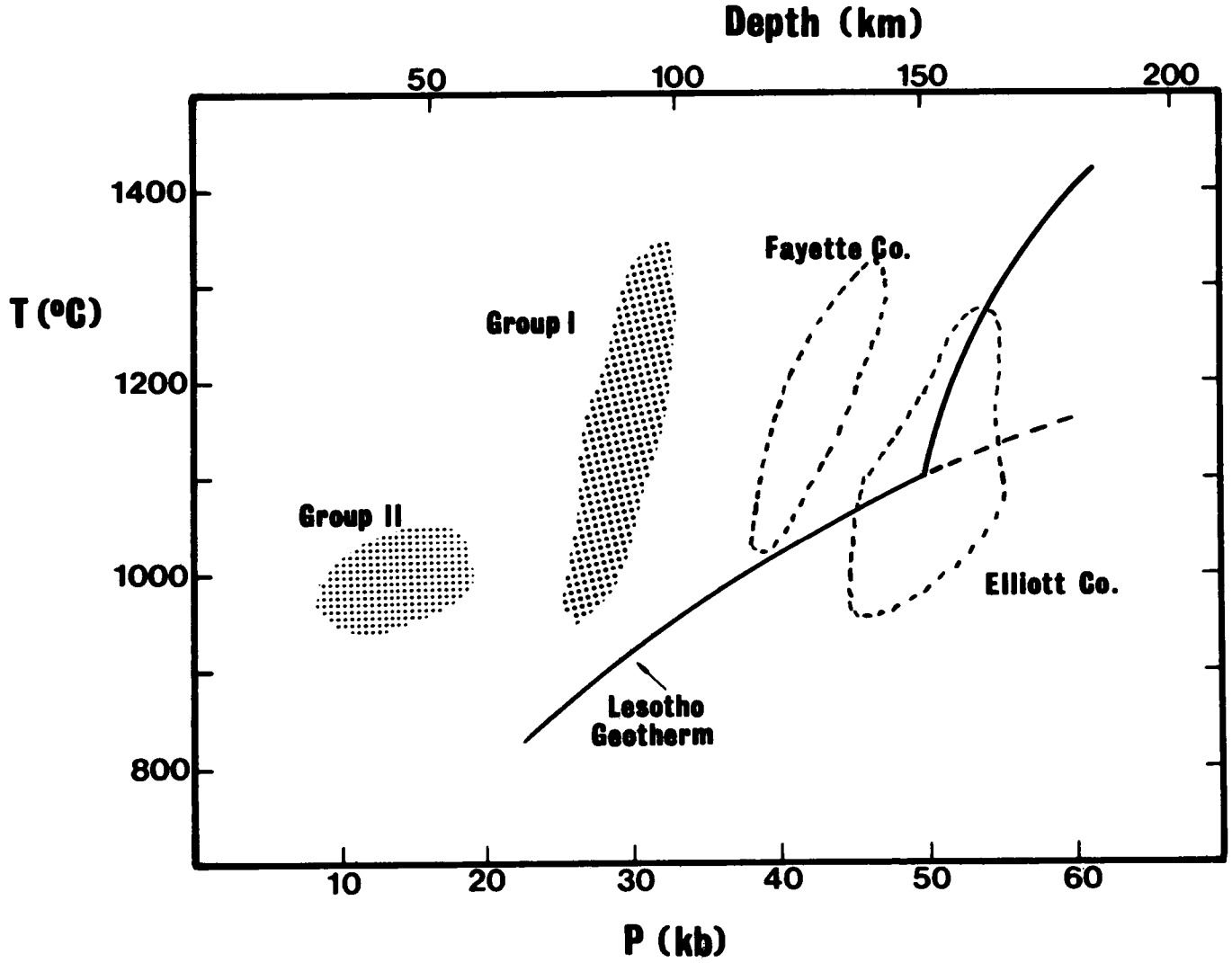
Depth (km)
50
100
150
200
1400
1200
1000
800
T (°C)
Group I
Group II
Fayette Co.
Elliott Co.
Lesotho
Geotherm
10
20
30
40
50
60
P (kb)

Figure 14.

CHAPTER V

DISCUSSION

The Taughannock Creek instrusives exhibit many of the characteristics commonly associated with kimberlites (see Chapter I). The rocks are inequigranular in texture and consist of minerals typically reported from kimberlite occurrences throughout the world. Moreover, the estimates of temperature and pressure of equilibration derived from some of these minerals (950 - 1350° C; 25 - 31 kb) are indicative of their crystallization at depths within the upper mantle (75 - 100 km). The chemical trends and textures observed in the spinels (reflecting late-stage increases in Ca and Ti activities) are also common characteristics of kimberlitic rocks (Haggerty et al., 1979; Pasteris, 1981).

Based on the above evidence, it is concluded that these rocks are kimberlitic; however, they are the products of magmatic processes originally active at depths shallower than those estimated for many other kimberlites in the eastern United States (140 - 200 km, Garrison and Taylor, 1980; Hunter and Taylor, 1982b) and other areas (e.g., Lesotho, Boyd and Nixon, 1975). Perhaps, as a result of its shallow depth of origin, the Taughannock Creek dikes are lacking in two phases frequently associated with other kimberlites; specifically, diamond and ilmenite. Pressure and temperature estimates from the megacryst suite imply equilibration outside the diamond stability field. The origin of ilmenite megacrysts in kimberlite has been the subject of considerable debate. It has been postulated that an

ilmenite concentration exists in the low velocity zone above areas of kimberlite genesis. Upon ascent, the kimberlitic melt encounters these cumulates of ilmenite and incorporates ilmenite megacrysts into the melt (e.g., Boyd and Nixon, 1973; Nixon and Boyd, 1973; Pasteris, 1980). The shallow depth of origin inferred for the Taughannock Creek kimberlite might have precluded the sampling of ilmenite cumulates located in the low velocity zone. Alternatively, some authors have proposed that ilmenite forms as a direct precipitate from the kimberlitic melt (e.g., Eggler et al., 1979; Gurney et al., 1979; Garrison and Taylor, 1980; Hunter and Taylor, 1982b). The paucity of ilmenite in the Taughannock Creek dikes could be an indication that the kimberlitic magma formed in a Ti-poor region of the mantle (possibly a function of depth), so that, despite fractionation, these Ti-poor melts never reached ilmenite saturation.

On the basis of petrographic, mineral chemistry, pressure and temperature constraints, three evolutionary stages can be recognized in the petrogenesis of the Taughannock Creek kimberlite (Figure 15). During Stage 1, a kimberlitic partial melt crystallized Group I minerals over a considerable depth and temperature interval within the upper mantle. Over the period of Stage 2, the rising kimberlitic melt subsequently penetrated and assimilated an ecologite body (Group II minerals) of lower crustal of shallow upper mantle origin. Finally, in Stage 3, the residual melt and crystallization products from both igneous bodies were emplaced as a hypabyssal-facies kimberlite.

Figure 15. Petrologic model of Taughannock Creek kimberlite showing three stages of evolution (see text for explanation).

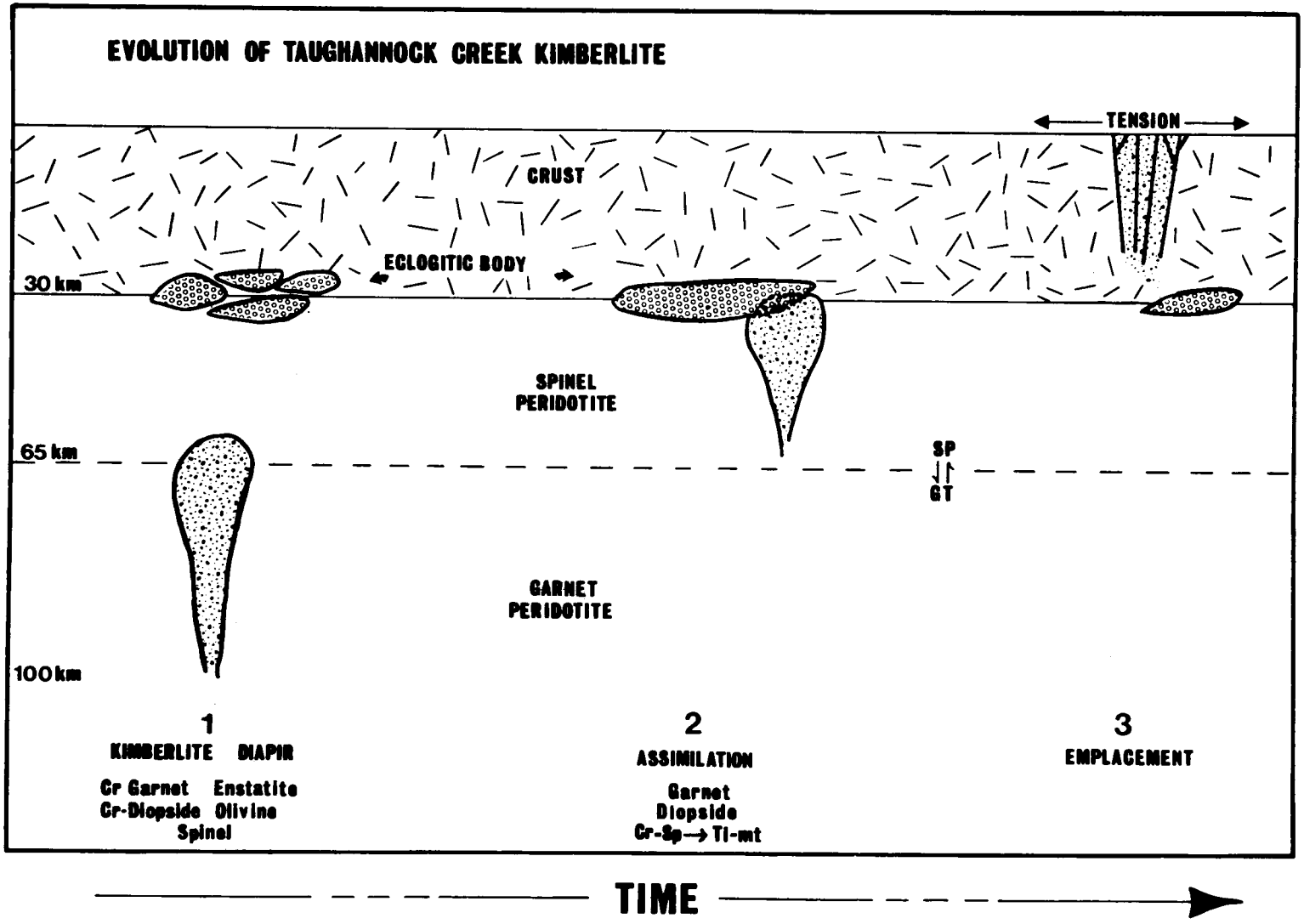
EVOLUTION OF TAUGHANNOCK CREEK KIMBERLITE
TENSION
CRUST
ECLOGITIC BODY
30 km
SPINEL
PERIDOTITE
65 km
SP
GT
GARNET
PERIDOTITE
100 km
1
KIMBERLITE DIAPIR
Cr Garnet Enstatite
Cr-Diopside Olivine
Spinel
2
ASSIMILATION
Garnet
Diopside
Cr-Sp→ Ti-mt
3
EMPLACEMENT
TIME

Figure 15.

Stage 1. The Group I megacrysts could have originated in two ways: (1) they could represent fragments of disaggregated mantle lherzolite that were assimilated into the kimberlitic magma as xenocrysts; (2) they could be direct precipitates from the kimberlitic melt. The latter possibility best explains the origin of Group I minerals because: (1) megacryst grain sizes are typically larger (0.4 - 1.2 cm) than those exhibited by lherzolite constituents; (2) none of these megacrysts show evidence of reaction with a melt (e.g., reaction rimming) as would be expected from xenocryst assimilation; (3) variations in Cr and Ti contents exhibited by Group I megacrysts imply their precipitation from an evolving liquid.

Thermal pertubations can induce partial melting in the mantle, resulting in melts of kimberlitic composition (Wyllie, 1980). Pressure and temperature estimates derived from Group I garnets and pyroxenes imply that these phases crystallized over a depth interval beginning at approximately 100 km (within the garnet stability field); these depths are compatible with the formation of kimberlitic melts (Eggler and Wendlandt, 1979; Wyllie, 1979; 1980). The high mg and Cr-contents of Group I garnets and pyroxenes are also compatible with crystallization in a mantle environment. The crystallization interval, as inferred from geothermobarometric data, extended into the spinel stability field (less than 65 - 75 km). The presence of garnet and spinel megacrysts and spinel peridotite nodules in the Group I assemblage also supports the conclusion that crystallization encompassed the stability fields of both garnet and spinel. Because high Cr-contents stabilize spinel crystallization into the garnet

field (e.g., MacGregor, 1970), Cr-spinel megacrysts and garnet actually may have co-precipitated over a portion of the crystallization interval.

Although Group I minerals exhibit a restricted range of mg values over the pressure and temperature range of Stage 1, there are variations in minor elements (e.g., Cr, Ti) that are indicative of fractional crystallization. This uniform mg of the kimberlitic magma may be controlled by fO_2. The fO_2 in kimberlite probably is buffered with decreasing temperature (e.g., Eggler, 1982) resulting in a near-constant Fe^{2+}/Fe^{3+}, thus permitting the fractionation of olivine, pyroxene, garnet, and spinel to lead to a decrease in mg with decreasing temperature. If fO_2 increased with decreasing temperature, relative to buffer curves, Fe^{2+}/Fe^{3+} in the melt would decrease, thus moderating the decrease in mg. More likely, the constant mg of the melt may be a function of a low crystal-melt ratio, allowing the bulk MgO content of the melt to be buffered by the composition of the surrounding peridotitic mantle.

Stage 2. During Stage 2 (Figure 15), the evolving kimberlitic melt penetrates and reacts with a lower crustal/upper mantle eclogitic body of unrelated origin. This interaction results in the incorporation of eclogitic minerals into the kimberlitic melt. Group II minerals present in the Taughannock Creek dikes are interpreted to be xenocrysts from the assimilated eclogite. It should be stressed that minerals of the Group II assemblage are genetically unrelated to the kimberlite.

The presence of plagioclase in eclogite nodules, together with temperature estimates derived from Group II minerals, indicate that

this assemblage crystallized in the lower crust or uppermost mantle (25 - 50 km in depth). Distinctly different from Group I, the Group II suite lacks olivine and enstatite and exhibits significantly lower Cr and higher Fe contents than those minerals identified with the kimberlitic melt (Group I). Systematic variations in Al_2O_3, TiO_2, and Na_2O imply that these minerals precipitated from a fractionating melt. Although it is a possibility that they were formed by exsolution, the intergrowths of garnet and clinopyroxene observed in eclogite nodules and in clinopyroxene megacrysts form textures interpreted to be the result of co-precipitation from a melt, perhaps in an analogous fashion to ilmenite/clinopyroxene intergrowths (Boyd and Nixon, 1973). The compositional similarity of Group II garnet and clinopyroxene megacrysts with these phases occurring as intergrowths is compelling evidence in favor of co-precipitation; it would be expected that the exsolution of garnet from clinopyroxene would deplete the pyroxene in Al_2O_3 relative to pyroxenes that had not exsolved an Al-rich phase. No such depletion has been observed. Additionally, the temperatures calculated from coexisting assemblages of clinopyroxene and garnet fall well within the range of temperatures estimated from discrete megacrysts, suggesting that intergrowth temperatures are not subsolidus. Finally, the textures exhibited by the nodular intergrowths are similar to textures produced experimentally in alloys by co-precipitation (Wyatt, 1977).

Subsequent to Stage 1, the kimberlitic melt disrupted the eclogite body, assimilating eclogitic crystallization products. Group II clinopyroxene xenocrysts exhibit reverse core-rim zonation in the

form of reaction rims that record decreases in TiO_2 and Na_2O and increases in mg and Cr_2O_3. These core to rim chemistries reflect the chemical modification of the eclogite phases via the intrusion of the kimberlitic melt. The absence of rims on kimberlitic clinopyroxenes suggests that the eclogite was present as a crystalline solid or a crystal-mush containing little melt.

Stage 3. During Stage 3 (Figure 15), the kimberlitic melt underwent final chemical evolution and was emplaced in its setting as dikes. The exact timing of the crystallization of groundmass phases is enigmatic. There is no petrographic evidence that uniquely associates groundmass crystallization with any one stage of development; it is possible that the groundmass phases crystallized concurrently with portions of all three stages. The paragenetic sequence Cr-spinel → Ti-magnetite → perovskite as observed in the groundmass, is typical of mid to late-stage melt evolution in kimberlites. The reaction of Cr-spinel with the melt to form Ti-magnetite records a decrease in Cr-activity and increases in Ti and Fe^{3+} activities within the melt. A late-stage increase in Ca-activity is reflected in the reaction of Ti-magnetite and the residual melt to form perovskite.

The crystallization of phlogopite is also difficult to precisely determine with respect of time; this problem is further complicated by the complex chemical relationships exhibited between large, zoned phlogopite crystals and smaller groundmass grains. On the basis of their Cr-poor cores, these larger phlogopites are interpreted to have crystallized from a non-kimberlitic melt; their subsequent incorporation

by the Cr-rich kimberlite during its ascent is recorded by the increases in Cr exhibited in the xenocryst rims. These rim compositions are compatible with groundmass phlogopite compositions, suggesting their co-precipitation. Furthermore, the inclusion of Cr-spinels within xenocryst rims and groundmass phlogopites is an indication that the crystallization of these two phases was at least partially concurrent.

The kimberlite was emplaced as narrow dikes (less than 0.5 m wide) intruded into flat-lying Devonian shales. The country rock exhibits little effects of thermal alteration, suggesting that the kimberlite was injected as a relatively cool, gas-charged fluid. The majority of other kimberlite occurrences in Central New York are also hypabyssal-facies intrusions, not explosively emplaced diatremes. Many diatremes narrow with depth, grading into feeder dikes (Dawson, 1967). It is possible that the lack of diatremes in this area is attributable to erosional processes which removed the upper portion of the kimberlite intrusions, leaving the feeder dikes exposed. Alternatively, the predominance of dikes could indicate that the kimberlite underwent non-explosive emplacement. This mode of emplacement could occur if the overlying country rock exerted resistance over the rising kimberlite, yielding to the intrusion only along pre-existing joint planes. Indeed, most of the kimberlite dikes in Central New York, including those exposed in Taughannock Creek, follow the dominant North-South trending joint pattern (Foster, 1970).

Crough et al. (1980) and Crough (1981) have proposed that the kimberlite occurrences in New York are related to thermal activity associated with the Great Meteor hotspot, a thermal upwelling active

during the early Jurassic. Although plausible in some respects, this theory becomes less cogent upon consideration of the great distances (500 km) that separate the kimberlite occurrences from the track of the hotspot. An alternative suggestion is that the kimberlites occurring along the Appalachian Plateau in the eastern U.S. are manifestations of thermal changes and tensional tectonics associated with the opening of the North Atlantic during Triassic-Jurassic time (e.g., Hunter and Taylor, 1982b; Taylor and Hunter, 1982). Parrish and Lavin (1982) cite evidence suggesting that kimberlites in the Appalachian Plateau are distributed along structure-parallel basement faults that may have been activated by tensional stress during the Mesozoic. The rifting episode could have initiated the development of cracks in the lower crust; volatile activity associated with the kimberlitic melt would have enhanced crack propagation, resulting in the emplacement of the kimberlite (Figure 15, page 55).

CHAPTER VI

SUMMARY

The petrography and mineralogy of the Taughannock Creek intrusives record three stages in the petrologic evolution of a kimberlite derived from a relatively shallow source. Initial crystallization of olivine, pyropic garnet, Cr-diopside and enstatite occurred at depths overlying the low velocity zone. Precipitation of these phases continued as the melt ascended to higher depths within the upper mantle. As the melt rose through the spinel stability field, it crystallized Cr-Al spinel megacrysts and incorporated spinel peridotite xenoliths. During Stage 2, the kimberlite melt encountered and assimilated the components of an unrelated eclogitic body situated near the base of the crust. This lower crustal/upper mantle body, consisting of garnet and clinopyroxene and minor plagioclase, was present as a crystalline solid or possibly as a crystal mush. Groundmass spinels and phlogopites may have crystallized at this time, although the exact time of their precipitation, relative to other phases, is not known. Textural and compositional relationships among phlogopites indicate the incorporation of a suite of non-kimberlitic phlogopites into the kimberlitic melt; textural relationships between phlogopite and Cr-spinels suggest that this event occurred prior to, or concurrent with, groundmass crystallization. In Stage 3 the kimberlite was intruded as dikes into the surrounding country rock. Both the genesis and emplacement of the kimberlite may have been controlled by tectonic events associated with the opening of the North Atlantic Ocean.

LIST OF REFERENCES

LIST OF REFERENCES

Agee, J.J., J.R. Garrison and L.A. Taylor (1982) Petrogenesis of oxide minerals in kimberlite, Elliott County, Kentucky. Am. Mineral., 67, 28-42.

Akella, J., and F.R. Boyd (1974) Petrogenic grid for garnet peridotites. Carnegie Inst. Wash. Yearb., 73, 269-273.

Albee, A.L. and L. Ray (1970) Correction factors for electron-probe microanalysis of silicates, oxides, carbonates, phosphates, and sulphates. Anal. Chem., 42, 1408-1414.

Barnett, V.H. (1905) Notice of a new dike at Ithaca, New York. Am. J. Sci., 19, 210.

Basu, A.R. and E. Rubury (1980) Tectonic significance of kimberlite dikes in central New York. Geol. Soc. Am. Abstracts with Programs, 12, 23.

Bence, A.E. and A.L. Albee (1968) Empirical correction factors for the electron microanalysis of silicates and oxides. J. Geol., 76, 383-403.

Boctor, N.Z. and F.R. Boyd (1980) Oxide minerals in the Liqhobong kimberlite, Lesotho. Am. Mineral., 65, 631-638.

Boctor, N.Z. and H.O.A. Meyer (1979) Oxide and sulphide minerals in kimberlite from Green Mountain, Colorado. In F.R. Boyd and H.O.A. Meyer, Eds., Kimberlites, Diatremes, and Diamonds: Their Geology, Petrology, and Geochemistry, 217-228.

Boyd, F.R. and P.H. Nixon (1973) Origin of the ilmenite-silicate nodules in kimberlites from Lesotho and South Africa. In P.H. Nixon, Ed., Lesotho Kimberlites, 254-268.

Boyd, F.R. and P.H. Nixon (1975) Origins of the ultramafic nodules from some kimberlites of northern Lesotho and the Monastery Mine, South Africa. Phys. Chem, Earth, 9, 431-454.

Clarke, D.B. and R.H. Mitchell (1975) Mineralogy and petrology of the Somerset Island kimberlite, N.W.T., Canada. Phys. Chem, Earth, 9, 123-135.

Crough, S.T. (1981) Mesozoic hotspot epeirogeny in eastern North America. Geology, 9, 2-6.

Crough, S.T., W.J. Morgan and R.B. Hargraves (1980) Kimberlites: their relation to mantle hotspots. Earth Planet. Sci. Lett., 50, 260-274.

Dawson, J.B. (1967) A review of the geology of kimberlites. In P.J. Wyllie, Ed., Ultramafic and Related Rocks, 241-251.

Dawson, J.B. (1980) Kimberlites and Their Xenoliths, 252 pp.

Dawson, J.B. and J.B. Hawthorne (1970) Intrusion features of some hypabyssal South African kimberlites. Bull. Volcanol., 34, 740-757.

Eggler, D.H. (1982) Mantle oxidation states: Evidence from olivine-orthopyroxene-ilmenite assemblages. EOS, Trans. Am. Geophys. Union, 63, 450.

Eggler, D.H., M.E. McCallum and C.B. Smith (1979) Megacryst assemblages in kimberlite from northern Colorado and southern Wyoming: Petrology, geothermometry-barometry, and areal distribution. In F.R. Boyd and H.O.A. Meyer, Eds., The Mantle Sample: Inclusions in Kimberlites and Other Volcanics, 183-196.

Eggler, D.H. and R.F. Wendlandt (1979) Experimental studies on the relationship between kimberlite magmas and partial melting of peridotite. In F.R. Boyd and H.O.A. Meyer, Eds., Kimberlites, Diatremes, and Diamonds: Their Geology, Petrology, and Geochemistry., 330-338.

Ehrenburg, S.N. and W.L. Griffin (1979) Garnet granulite and associated xenoliths in minette and serpentinite diatremes of the Colorado Plateau. Geology, 7, 483-487.

Foster, B.P. (1970) A study of the kimberlite-alnoite dikes in central New York. M.S. thesis, State University of New York at Buffalo, 55 pp.

Garrison, J.R. and L.A. Taylor (1980) Megacrysts and xenoliths in kimberlite, Elliott County, Kentucky: A mantle sample from beneath the Permian Appalachian Plateau. Contrib. Mineral. Petrol., 75, 27-42.

Garrison, J.R. and L.A. Taylor (1981) Petrogenesis of pyroxene-oxide intergrowths from kimberlite and cumulate rocks: Co-precipitation or exsolution? Am. Mineral., 66, 723-740.

Green, D.H. and A.E. Ringwood (1967) The stability fields of aluminous pyroxene peridotite and garnet peridotite and their relevance in upper mantle structure. Earth Planet. Sci. Lett., 3, 151-160.

Griffin, W.L., D.A. Carswell and P.H. Nixon (1979) Lower crustal granulites and eclogites from Lesotho, southern Africa. In F.R. Boyd and H.O.A. Meyer, Eds., The Mantle Sample: Inclusions in Kimberlites and Other Volcanics, 59-86.

Gurney, J.J., W.R.O. Jakob and J.B. Dawson (1979) Megacrysts from the Monastery kimberlite pipe, South Africa. In F.R. Boyd and H.O.A. Meyer, Eds., The Mantle Sample: Inclusions in Kimberlites and Other Volcanics, 227-243.

Haggerty, S.E. (1976) Opaque mineral oxides in terrestrial igneous rocks. In D. Rumble, Ed., Oxide Minerals, Hg101-Hg300.

Haggerty, S.E., R.B. Hardie and B.M. McMahon (1979) The mineral chemistry of ilmenite nodule associations from the Monastery diatreme, In F.R. Boyd and H.O.A. Meyer, Eds., The Mantle Sample: Inclusions in Kimberlites and Other Volcanics, 249-256.

Harte, B. and J.J. Gurney (1975) Evolution of clinopyroxene and garnet in an eclogite nodule from the Roberts Victor kimberlite pipe, South Africa. Phys. Chem. Earth., 9, 367-387.

Hunter, R.H. and L.A. Taylor (1982a) Instability of garnet from the mantle: Glass as evidence of metasomatic melting. Geology, (in press).

Hunter, R.H. and L.A. Taylor (1982b) Magma mixing in the evolution of kimberlite: Petrogenesis of megacrysts and inclusions in the Fayette County kimberlite, Pennsylvania. Am. Mineral. (submitted).

Jackson, D.E., R.H. Hunter and L.A. Taylor (1982a) A Mesozoic window into the sub-Appalachian mantle: Kimberlite from the eastern United States. Geol. Soc. Am. Abstracts with Programs, 14, 28.

Jackson, D.E., R H. Hunter and L.A. Taylor (1982b) Shallow-level kimberlite from the northeastern U.S.A.: An unusual mantle sample. EOS, Trans. Am. Geophys. Union, 63, 463-464.

Kemp, J.F. (1891) Peridotite dikes in the Portage sandstone near Ithaca, New York. Am. J. Sci., 42, 410-412.

Kissling, R.D., R.H. Hunter and L.A. Taylor (1981) A petrologic assessment of the oxide phases from a kimberlite in the Appalachian Plateau of Pennsylvania. EOS, Trans. Am. Geophys. Union, 62, 414.

Lindsley, D.H. (1980) Phase equilibria of pyroxenes at pressures >1 atmosphere. In C.T. Prewitt, Ed., Pyroxenes, 289-307.

Lindsley, D.H. and S.A. Dixon (1976) Diopside-enstatite equilibria at 850° C to 1,400° C, 5 kb. Am. J. Sci., 276, 1285-1301.

Lindsley, D.H., J.E. Grover and P.M. Davidson (1981) The thermodynamics of the $Mg_2Si_2O_6$ - $CaMgSi_2O_6$ join: A review and a new model. In S.K. Saxena, Ed., Advances in Physical Geochemistry.

Lovering, J.F. and A.J.R. White (1964) The significance of primary scapolite in granulitic inclusions from deep-seated pipes. J. Petrol., 5, 195-218.

MacGregor, I.D. (1970) The effect of CaO, Cr_2O_3, Fe_2O_3 and Al_2O_3 on the stability of spinel and garnet peridotites. Phys. Earth Planet. Interiors, 3, 372-377.

MacGregor, I.D. (1974) The system $MgO-Al_2O_3-SiO_2$: Solubility of Al_2O_3 in enstatite for spinel and garnet peridotite compositions. Am. Mineral., 59, 110-119.

MacGregor, I.D. (1979) Mafic xenoliths from the Kao kimberlite pipe. In F.R. Boyd and H.O.A. Meyer, Eds., The Mantle Sample: Inclusions in Kimberlites and Other Volcanics, 156-172.

Martens, J.H.C. (1924) Igneous rocks of Ithaca, New York and vicinity. Geol. Soc. Am. Bull., 35, 305-320.

Matson, G.C. (1905) Peridotite dikes near Ithaca, New York. J.Geol., 13, 264-275.

Maynard, J.E. and L.W. Polger (1946) A study of the Salt Springs Road peridotite dike in Syracuse, New York. Am. Mineral., 31, 471-485.

McGee, E.S. and B.C. Hearn (1982) Lake Ellen kimberlite, northern Michigan: Thermobarometry of mantle inclusions: EOS, Trans. Geophys. Union, 63, 463.

Meyer, H.O.A. (1976) Kimberlites of the continental United States: A review. J. Geol., 84, 377-403.

Nixon, P.H. and F.R. Boyd (1973) The discrete nodule (megacryst) association in kimberlites from northern Lesotho. In P.H. Nixon, Ed., Lesotho Kimberlites, 67-75.

Parrish, J.B. and P.M. Lavin (1982) Tectonic model for kimberlite emplacement in the Appalachian Plateau of Pennsylvania. Geology, 10, 344,347.

Pasteris, J.D. (1980) The significance of groundmass ilmenite and megacryst ilmenite in kimberlites. Contrib. Mineral. Petrol., 75, 315-325.

Pasteris, J.D. (1981) Kimberlites: Strange Bodies? EOS, Trans. Am. Geophys. Union, 62, 713-716.

Perkins, D., T.J.B. Holland and R.C. Newton (1981) The Al_2O_3 contents of enstatite in equilibrium with garnet in the system MgO - Al_2O_3 - SiO_2 at 15-40 kb and 900° C - 1600° C. Contrib. Mineral. Petrol., 78, 99-109.

Pimental, N, M. Bikerman and N.K. Flint (1975) A new K-Ar date on the Masontown dike, southwestern Pennsylvania. Penn. Geologist, 6, 5-7.

Schulze, D.J. and H.H. Helmstaedt (1978) Pyroxene-ilmenite intergrowths in garnet pyroxenite xenoliths from a New York kimberlite and Arizona latites. Am. Mineral., 63, 258-265.

Skinner, E.M.W. and C.R. Clement (1979) Mineralogical classification of southern Africa kimberlites. In F.R Boyd and H.O.A. Meyer, Eds., Kimberlites, Diatremes, and Diamonds: Their Geology, Petrology, and Geochemistry, 129-139.

Smith, J.V., R. Brennesholtz and J.B. Dawson (1978) Chemistry of micas from kimberlites and xenoliths: I. Micaceous kimberlites. Geochim. Cosmochim. Acta, 42, 959-971.

Smith, J.V. and J.B. Dawson (1975) Chemistry of Ti-poor spinels, ilmenites and rutiles from peridotite and eclogite xenoliths. Phys. Chem. Earth, 9, 309-322.

Snedden, W.T. and S.M. Kay (1981a) Initial stages of kimberlite eruption: Evidence from mantle minerals in the Ithaca kimberlites. Geol. Soc. Am. Abstracts with Programs, 13, 551.

Snedden, W.T. and S.M. Kay (1981b) Mineral chemistry of kimberlites and included xenoliths, Ithaca, New York. Geol. Soc. Am. Abstracts with Programs, 13, 178.

Taylor, L.A. and R.H. Hunter (1982) Kimberlites in the eastern United States: Location and depths of origin related to Mid-Atlantic tectonism. Abstract presented to Third International Kimberlite Conference, France, 1982.

Vanuxem, L. (1842) Geology of the Third District (final report). Natural History of New York, 169 pp.

Wood, B.J. (1974) Solubility of alumina in orthopyroxene coexisting with garnet. Contrib. Mineral. P trol., 46, 1-5.

Wyatt, B.A. (1977) The melting and crystallization behavior of a natural clinopyroxene-ilmenite intergrowth. Contrib. Mineral. Petrol., 61, 1-9.

Wyllie, P.J. (1979) Kimberlite magmas from the system peridotite-CO_2 - H_2O. In F.R. Boyd and H.O.A. Meyer, Eds., Kimberlites, Diatremes, and Diamonds: Their Geology, Petrology, and Geochemistry, 319-329.

Wyllie, P.J. (1980) The origin of kimberlite. J. Geophys. Res., 85, 6902-6910.

Zartmann, R.E., M.R. Brock, A.V. Heyl and H.H. Thomas (1967) K-Ar and Rb-Sr ages of some alkaline intrusive rocks from the central and eastern United States. Am. J. Sci., 265, 848-870.

VITA

David Ernest Jackson was born on 1 October 1956 in Nashville, Tennessee. He graduated from David Lipscomb High School in June, 1974.

Mr. Jackson entered The University of Tennessee, Knoxville in September, 1974 and graduated with a B.A. in Geology in 1978. Following employment as a field geologist with the Union Carbide Corporation he entered graduate school at The University of Tennessee in September, 1980. A portion of his graduate tenure was supported by a Graduate Teaching Assistantship from the Department of Geological Sciences. Upon the completion of studies toward the Master of Science degree, Mr. Jackson will be employed as a Petroleum Geologist by the Exxon Company in Kingsville, Texas. He is a member of Sigma Gamma Epsilon (geologic honorary) and the American Geophysical Union.

The author is married to Brenda J. Morgan, formerly of South Haven, Michigan.